

## Chapter 4

## Sorting out Compositional Trends in Sedimentary Rocks of the Bradbury Group (Aeolus Palus), Gale Crater, Mars

Kirsten L. Siebach, Michael B. Baker, John P. Grotzinger, Scott M. McLennan, Ralf Gellert, and Joel A. Hurowitz

### Key Points

- *Curiosity* obtained bulk chemistry for sedimentary rocks in the Bradbury group
- Coarse-grained rocks are enriched in plagioclase
- Geochemical trends are consistent with mineral sorting during transport

### Abstract

The compositional variations between sedimentary rocks analyzed by the *Curiosity* rover on the floor of Gale Crater are consistent with hydrodynamic sorting of mineral grains during transport from a relatively homogeneous basaltic provenance. During an 860-sol traverse across 9.5 km of the floor of Gale Crater, *Curiosity* obtained bulk chemistry measurements of over 100 fluvio-lacustrine sedimentary rocks in the Bradbury group using the Alpha Particle X-ray Spectrometer. These sedimentary rock compositions represent the set of source rock compositions altered by weathering, sorted by transport, and cemented during diagenesis. The Bradbury group samples are uniquely suited for sedimentary provenance analysis because they experienced negligible cation-loss, or open system chemical weathering, and their compositions can be modeled as sums of primary unaltered basaltic minerals using a Monte-Carlo model constrained by in-situ analyses. These samples were divided into seven categories based on grain size and texture, revealing that the coarse-grained textures are enriched in  $\text{Al}_2\text{O}_3$ ,  $\text{SiO}_2$ , and  $\text{Na}_2\text{O}$  and the fine-grained textures are enriched in mafic components. Geochemical and mineralogical modeling shows that the variation between grain sizes is correlated to addition or depletion of plagioclase minerals relative to mafic minerals. The presence of a  $\text{K}_2\text{O}$ -rich stratigraphic interval within the Bradbury group shows that one other distinctive protolith contributed

to basin fill. However, the dominant compositional trends are defined by mineral sorting consistent with hydrodynamic sorting of coarse plagioclase grains and fine mafic fragments from breakdown of a porphyritic basaltic provenance during transport into Gale Crater.

## 4.1 Introduction

Sedimentary rocks are repositories for detrital grains that are derived from all rock types present in their watersheds, altered by weathering, sorted by transport processes, and cemented by diagenetic fluids. The Mars Science Laboratory rover, *Curiosity*, has shown that Gale Crater preserves remnants of originally significant volumes of sedimentary rock, creating both the modern floor of the crater (Aeolus Palus) and the 5-km tall stack of sediments in the middle of the crater that makes up Mount Sharp (Aeolus Mons) [Grotzinger *et al.*, 2015]. As of sol 860, *Curiosity* had traversed across 9.5 km of the crater floor and covered over 65 vertical m of stratigraphy dominated by lithified fluvial deposits known as the Bradbury group [Grotzinger *et al.*, 2015]. These sedimentary deposits are invaluable tools for understanding the nature and variety of rock types in the Noachian-era terrain that makes up the region around Gale Crater and which was eroded to produce the material that filled the crater basin. However, deriving provenance information from bulk compositions of sedimentary rocks requires accounting for weathering, transport, alteration, and cementation processes that could modify the sedimentary rock compositions relative to their sources.

The bulk compositions of sedimentary rocks are significantly simpler to relate to the compositions of their source rocks if no open-system chemical alteration — i.e., changes in the bulk chemistry related to preferential leaching or retention of select elements — has occurred due to initial weathering of bedrock source regions or due to later diagenesis during sediment burial. A useful tool for measuring the extent of open system chemical alteration with only compositional data in terrestrial and martian sediments is the Chemical Index of Alteration (CIA), a ratio of  $\text{Al}_2\text{O}_3$  to labile cations designed as a chemical proxy for the degree of alteration of feldspars [Nesbitt and Young, 1982; 1984; McLennan *et al.*, 2014]. CIA values for Aeolus Palus are uniformly low, below even those values associated with incipient weathering, and the sediments fall within unaltered basalt

compositions on a mafic ternary diagram, indicating that chemical alteration of these sediments has been cation-conservative at the scale of the bulk chemistry [e.g. *McLennan et al.*, 2014]. Based on this evidence, we proceed with the simplest interpretation of the CIA data, that there was no significant open-system weathering in Aeolus Palus sediments. Assumptions inherent to this model are discussed further below.

In the assumed absence of open system chemical weathering, there are three significant components that contribute to the composition of sedimentary rocks: (1) the source rocks in the watershed, (2) erosion and transport processes that sort detrital and mineral grains by size and density [*Fedo et al.*, 2015], and (3) addition of diagenetic cements [*McLennan et al.*, 2003; *Nesbitt*, 2003]. Each of these contributors must be considered as a possible source of compositional change before implications of compositional deviations can be assessed.

- (1) The source rocks contributing to a watershed vary with space and time. Erosion is not uniform in space or time and can cause variations in the proportional contributions of different exposed rock units, and/or exposure of new rock units. For the Bradbury group, this problem is made tractable by (a) uniformly low CIA values, indicating that all or the large majority of contributing source rocks are primary basaltic rocks, with each reflecting equilibrium petrologic constraints [*Nesbitt and Young*, 1982; 1996], and (b) a series of measurements of rocks at different stratigraphic heights, allowing the ebb and flow of distinctive units to be traced [e.g. *Nesbitt and Young*, 1982; *Fedo et al.*, 1997].
- (2) Rock breakdown [*Fedo et al.*, 2015] and transport [*Frihy et al.*, 1995; *Ferguson et al.*, 1996; *Nesbitt and Young*, 1996; *Komar*, 2007] processes have long been known to sort minerals and lithic fragments by size and density [*Mackie*, 1923]. Initial erosion/breakdown tends to isolate phenocryst minerals and can segregate other minerals based on erodibility [*Nesbitt and Young*, 1996; *Fedo et al.*, 2015]. Transport processes further sort both mineral grains and lithic fragments by density and size, sometimes well enough to create heavy mineral placers of economic significance [*Frihy et al.*, 1995; *Hughes et al.*, 2000]. These processes strongly affect the relationship between the sedimentary rock compositions and the source

rock compositions, and can be assessed by comparison of the sedimentary rock compositions with their grain sizes and depositional environments.

- (3) Lithification of sedimentary rock typically involves physical compaction and chemical cementation by oversaturated groundwater fluids that interact with the sediments after they are deposited and precipitate minerals in the intergranular space [Worden and Burley, 2003]. Compaction alone does not change rock composition, but cementing interactions with groundwater fluids can alter the initial sediment composition by cement addition or by chemical alteration (dissolution and leaching of minerals in the detrital grains). Low CIA values likely indicate that diagenetic fluids did not significantly alter the compositions of the Gale Crater rocks, but possible addition of diagenetic cements must be carefully assessed by looking for compositional gradients or elemental enrichments within the rock suite. Cementation is assured for Bradbury rocks owing to their high degree of lithification and small amounts of residual porosity.

More than 100 measurements of the bulk compositions of outcrop and float rocks, taken by the Alpha Particle X-ray Spectrometer (APXS) instrument onboard *Curiosity*, provide a compositional dataset spanning a significant range of the rock textures and compositions present within Aeolus Palus. This study aims to use the compositions of the rocks observed by *Curiosity* to constrain a reasonable range of each of these effects, with implications for the range of contributing basaltic provenances and the extent of aqueous diagenesis.

## 4.2 Geologic Context

Gale Crater is a 155 km diameter crater sitting on fluvially dissected Noachian terrain on the Martian topographical dichotomy boundary. Crater counts of the ejecta blanket indicate that the impact occurred 3.8-3.6 Gya. Perhaps the most dominant feature of Gale crater is the 5-km-tall stack of sediments forming the crescent-shaped Mount Sharp (Aeolus Mons) in the center of the crater [Malin and Edgett, 2000]. This stack of sediments includes layers that were correlated with phyllosilicate and sulfate mineral detections in

orbital spectroscopy datasets, and motivated the selection of Gale Crater as the landing site for the *Curiosity* rover [Anderson and Bell, 2010; Milliken et al., 2010].

Comparisons between Gale and other complex craters of its size indicate that Mount Sharp is constructed around a tall central peak and the modern floor of Gale Crater is likely underlain by 1-2 km of sedimentary rock [Grotzinger et al., 2015]. This and other work with infilled craters suggests that much of the crater was once filled with sediments, and the current topography is based on eolian erosion of the “moat” around the central peak/Mount Sharp complex [Malin and Edgett, 2000; Farley et al., 2014; Grotzinger et al., 2015]. This hypothesis implies that sedimentary rocks in the “moat” (Bradbury group) may be genetically related to the lowest exposed layers in Mount Sharp [Grotzinger et al., 2015].

The *Curiosity* rover landed at Bradbury Rise, a topographic high within Aeolus Palus about 9 km from the geologic contact between the Bradbury group and Murray formation (Figure 4.1), and explored ~61 m of the Bradbury group stratigraphy. Lacustrine mudstones were discovered at the base of the stratigraphic section in Yellowknife Bay and also in the Murray formation at Pahrump Hills. The bulk of the intervening Bradbury group comprises a series of pebbly sandstones, conglomerates, and siltstone sedimentary rocks of fluvio-deltaic origin (Figure 4.1) [Grotzinger et al., 2015]. While some large conglomerate clasts and float rocks are potentially igneous in composition, the observed stratigraphic sequence of in-place rocks in Aeolus Palus is composed exclusively of sedimentary rocks. All measured beds within this portion of the traverse are approximately horizontal, so we will assume that elevation is a good proxy for stratigraphic position within these units [Grotzinger et al., 2014; Grotzinger et al., 2015].

## **4.3 Methods**

### **4.3.1 APXS**

The Alpha-Particle X-ray Spectrometer (APXS) instrument mounted on *Curiosity*'s robotic arm enables in-situ X-ray spectroscopy, providing the average composition of a sample within a 1.7 cm diameter circle. The instrument uses X-rays produced by a  $^{244}\text{Cm}$  source and the penetration depth varies between 2 to 80  $\mu\text{m}$  for reported elements between

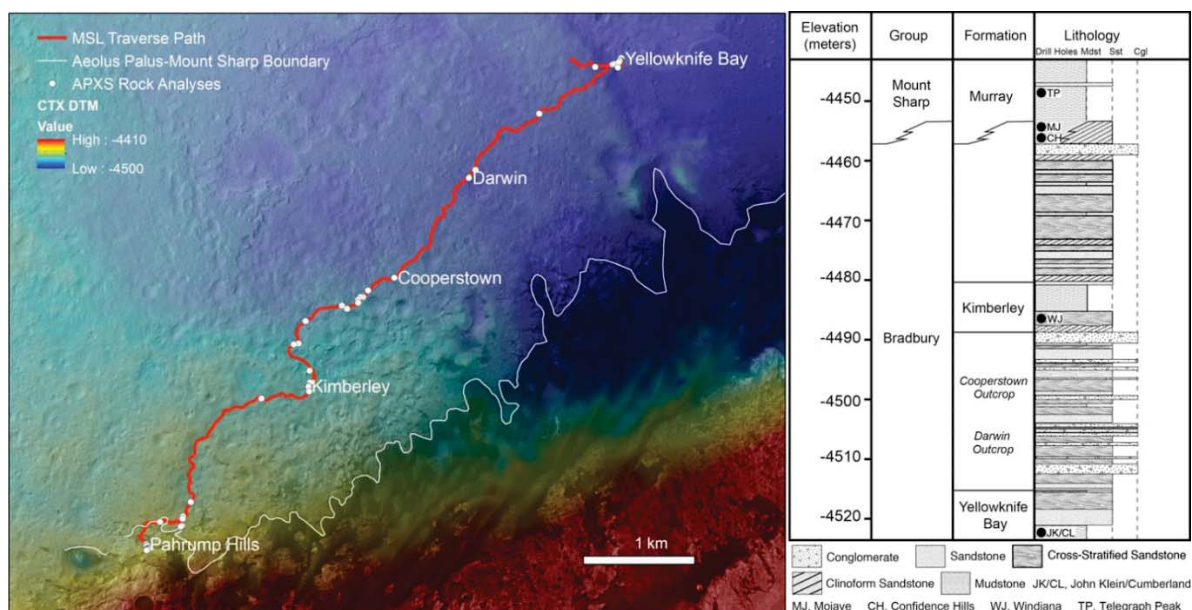


Figure 4.1 Overhead Map of *Curiosity* Traverse and APXS Locations

Overhead map showing the location and climbing elevation of the 9.5 km traverse path of the *Curiosity* rover during the first 860 sols after landing, with the stratigraphic column over the same portion of the traverse (based on elevation) on the right. Major outcrops labeled. Rover traverse begins west of Yellowknife Bay, jogs east to Yellowknife Bay, and then continues to the southwest. Locations of APXS analyses marked with white dots. White line on map represents main transition from Aeolus Palus (Bradbury group) rocks to Mount Sharp group rocks at the Pahrump Hills outcrop, reached on sol 750, although these facies are interfingered as shown in stratigraphic column.

Na and Fe, increasing with elemental mass. The intensity of characteristic X-ray energy responses from each element based on particle-induced X-ray emission and X-ray fluorescence is used to quantify elemental abundances for major elements and some trace elements [Gellert *et al.*, 2009; Campbell *et al.*, 2012; Gellert and Clark, 2015]. Regularly reported oxides and trace elements are (wt%): Na<sub>2</sub>O, MgO, Al<sub>2</sub>O<sub>3</sub>, SiO<sub>2</sub>, P<sub>2</sub>O<sub>5</sub>, SO<sub>3</sub>, Cl, K<sub>2</sub>O, CaO, TiO<sub>2</sub>, Cr<sub>2</sub>O<sub>3</sub>, MnO, FeO<sub>T</sub>, and (ppm): Ni, Zn, Br. Reported errors are statistical (2σ) errors based on the measurement duration, standoff distance, and temperature as reflected in the spectrum fitting routine, not errors associated with the instrument calibration. See Campbell *et al.* for more details on the instrument calibration and estimates of analytical accuracy [Campbell *et al.*, 2012].

APXS data are frequently normalized to remove volatile elements SO<sub>3</sub> and Cl (but not lighter elements) in order to correct for dust cover [Rieder *et al.*, 1997; Schmidt *et al.*, 2014]. This may be problematic if there is SO<sub>3</sub> or Cl in the rocks themselves or if there are excess light elements in the dust, and there is evidence that Martian magmas may be slightly enriched in sulfur and chlorine relative to terrestrial magmas [Dreibus and Wanke, 1985; Filiberto and Treiman, 2009], but it is a simple first-order correction. Here, we use sulfur- and chlorine-free normalization for mineral modeling. In element-element diagrams, in order to acknowledge the presence of dust but avoid assumptions about the dust and rock composition, we calculated the average weight percent that would have been removed had we normalized without SO<sub>3</sub> and Cl (avg SO<sub>3</sub> + avg Cl = 6%) and used this weight percent to make an acceptable error envelope around modeled predictions to compare to observations. This enables the reader to see the original measured APXS data, and the envelope surrounding an average dust-cover window without assuming any specific dust composition.

APXS targets are often analyzed under multiple conditions in order to obtain the most information possible from a contact science stop with the rover for that target. The same target spot may be analyzed at multiple times of day in order to work around planning schedules. A raster across the rock may analyze up to ~5 overlapping spots on a heterogeneous rock in order to constrain the compositions of the various components observed. A target may be analyzed as-is and then either analyzed with the ChemCam

instrument (the shock front produced by the LIBS technique frequently removes dust) or brushed with the dust removal tool (DRT), and then analyzed with the APXS instrument again with less dust cover. In some cases, the target was analyzed only after dust removal. If a target was drilled, the drill tailings adjacent to the hole were analyzed, as well as the discarded sample processed by sieving. For targets within the Bradbury group, 112 APXS analyses were completed on or offset from 73 distinct named rock targets. The DRT was only used on 8 distinct named targets. For this study, in order to capture the variation between rock surface textures most completely, we include observations both before and after dust removal as distinct observations. In cases where the same target was analyzed at multiple times of day, we use only the observation with the longest integration time (or best distance to target and thermal conditions), judged by the smallest reported statistical error associated with the measurement. Overlapping, or ‘offset’ targets are typically included, because variability occurs on short distance scales, but these are excluded to minimize bias in some plots (labeled as ‘offset targets excluded’).

#### 4.3.2 MAHLI

The Mars Hand Lens Imager (MAHLI) instrument is a high-resolution focusing color camera mounted on *Curiosity*’s robotic arm. It can focus between  $\sim 2.1$  cm and infinity and is typically used for high-resolution ( $14+$   $\mu\text{m}/\text{pixel}$ ) imaging of targets of interest, including all APXS targets [Edgett *et al.*, 2012]. For this study, the MAHLI images taken with  $\sim 5$  cm standoff distance ( $\sim 30$   $\mu\text{m}/\text{pixel}$ ) for each of the APXS targets were used for initial textural comparison. In the few cases where such imagery was not taken, higher standoff distances or images from the Mastcam were used to determine textures. For some targets, higher resolution imagery was also available and this was used whenever possible to clarify grain sizes and compare textures.

## 4.4 Results

### 4.4.1 Rock Classification by Texture

The classification of detrital sedimentary rocks is typically based on the sizes of the grains within the rock. On Mars, grain size assessment can be complicated because of several reasons: first, the MAHLI resolution limit at a typical standoff distance is  $\sim 30 \mu\text{m}/\text{px}$ , so only distinctive grains larger than  $\sim 50\text{-}100 \mu\text{m}$  are distinguishable; second, the in-situ rock surfaces are frequently dust-covered, obscuring grain boundaries; and third, many of the targets *Curiosity* has observed have extremely homogeneous coloring, making it even more difficult to clearly distinguish grains from cement or matrix. Therefore, for the collection of targets that MSL analyzed with APXS and MAHLI in the first 860 sols, the classification system defined here was based on grain size wherever possible, surface texture and coloring when grain sizes could not be distinguished, and the two mudstone formations (Sheepbed mudstone of the basal Bradbury group and Murray formation mudstone of the Mount Sharp group exposed in the Pahrump Hills) were separated by stratigraphic group. Samples with clear diagenetic overprinting (e.g. nodular and dendritic concretions, fracture fills) were further split into their own category. In total, eight textural classes were identified to encompass the range of MAHLI and APXS targets observed by *Curiosity* in the first 860 sols: Sheepbed mudstone (Figure 4.2a), fine sandstone (Figure 4.2b), sandstone (Figure 4.2c), conglomerate (Figure 4.2d), uncertain (Figure 4.2e), possible igneous (Figure 4.2f), diagenetic (Figure 4.2g), and Murray mudstone (Figure 4.2h). Each of these textural classes is described in detail below:

*Sheepbed Mudstone.* (n = 10, Figure 4.2a) The Sheepbed mudstone member is the lowermost stratigraphic unit of the Yellowknife Bay formation, described in detail in Grotzinger et al (2014). The rock texture in this unit was extremely smooth at the MAHLI resolution (up to  $15 \mu\text{m}/\text{pixel}$ ). There were a variety of diagenetic targets within this unit (n=20) where we examined concretions, raised ridge features, and/or light-toned veins, which were categorized as diagenetic targets and excluded from the Sheepbed mudstone category. Several of the observations in this category were on dusty surfaces.

*Fine Sandstone.* (n = 15, Figure 4.2b) The fine sandstone category includes observations of sandstones or siltstones with grain sizes approximately at the MAHLI limit

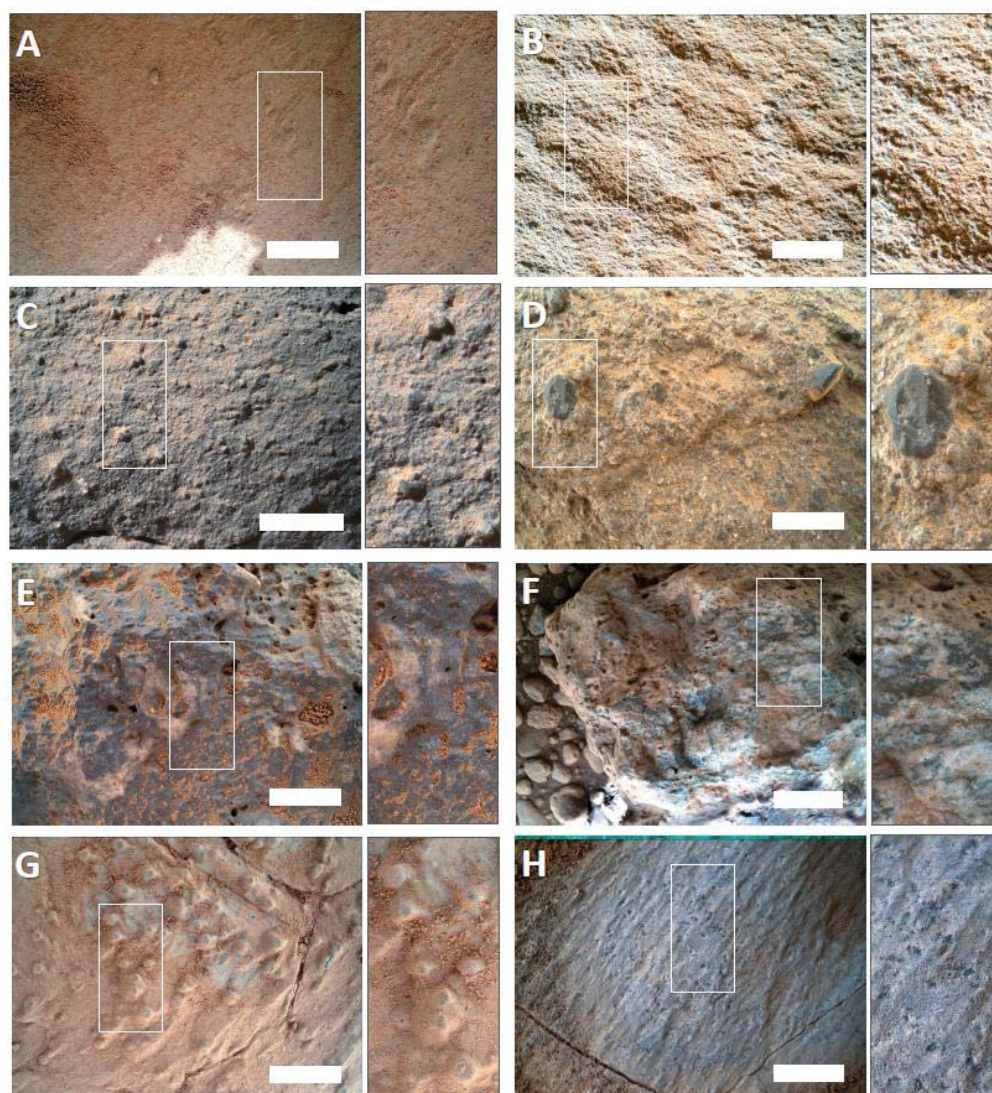


Figure 4.2 MAHLI Image Examples of Textural Classification Scheme

Examples of each of the textural classes of rocks in the Bradbury group (a-g) and the Murray mudstone in the Mount Sharp group (h). White scale bars are 1 cm across. Classes were divided on the basis of grain size and/or surface texture and coloring, and include: (a) Sheepbed mudstone (n=10), exposed in Yellowknife Bay with grains finer than the limit of resolution, (b) Fine Sandstone (n=15), well-sorted siltstones to sandstones, (c) Sandstone (n=24), medium to pebbly sandstones, (d) Conglomerate (n=15), primary grain sizes >1 mm, rounded grains, clasts up to 6 cm, (e) Uncertain (n=15), float rocks with poorly-defined grain boundaries, sometimes weather like conglomerates (f) Possible Igneous (n=4), small group of float rocks and one clast in a conglomerate with porphyritic textures like igneous diorites (g) Diagenetic (n=39), rocks with clearly diagenetic textures including preferential cementation and fracture fills, and (h) Murray Mudstone (n=27), mudstone observed at Pahrump Hills in Mount Sharp group, fine-grained with potential secondary crystal structures.

of resolution. These are all well-sorted siltstones to fine sandstones and do not have visible grains larger than  $\sim 200 \mu\text{m}$ .

*Sandstone* (n = 24, Figure 4.2c) The sandstone category includes observations of medium grained, sometimes pebbly, sandstones that are primarily composed of  $<0.5 \text{ mm}$  grains. These grains (exclusive of sparse pebbles) range from well-sorted to poorly-sorted. Void space mapping in these samples indicated that apparent primary porosity is quite low, so these samples were well cemented, although some secondary porosity is apparent (potentially because of surface weathering). Where pebbly, clasts range up to a centimeter in diameter and are dispersed in the sandstone matrix.

*Conglomerate* (n = 15, Figure 4.2d) Conglomerate targets include those targets with primary grain sizes  $>1 \text{ mm}$ . These are typically poorly sorted and show variable cementation, both within a given outcrop and across the traverse. Some of these targets have significant dust cover. Individual clasts, where identifiable and not dusty, range from light-toned to dark-toned, and from sub-angular to sub-round. The largest clasts are up to 6 cm across. Endmembers of this class range from variably-cemented rocks with clearly identifiable grains (e.g. Mount Bastion sol 399, Bardin Bluffs sol 394) to well-cemented conglomerates that are more homogeneous in color but have a vuggy surface texture from weathering that reveals clast boundaries (e.g. Oneida sol 506, Jum Jum sol 550).

*Uncertain* (n = 15, Figure 4.2e) The uncertain category contains a subset of float rocks whose dust cover and weathering textures make it difficult to define any grain boundaries, indicating that either the grains are below the resolution limit of the image or they are well-cemented and relatively homogeneous in color. A number of rocks in this category have some weathering textures or color changes that hint at the presence of larger grains, but these are not well-defined. Some of these rocks look very similar to the well-cemented conglomerates with homogeneous surface color, but they are assigned to this category because the grain boundaries are not defined and their context is uncertain because they are float rocks (e.g. Nedrow, sol 503; Kodak, sol 512; Monkey Yard, sol 564). Other rocks in this category show some variability in color, including several-mm light-toned patches that blend back into the dark grey rock, but the colors blend together instead of creating sharp grain boundaries (e.g. Morehouse, sol 503; Lowerre and Larrabee, sol 510).

Finally, a few rocks in this category do not show any clear evidence for visible grains, and may be quite fine-grained. These tend to weather with a vuggy texture that further obfuscates their origin. Some of these have been categorized by other authors in dramatically different ways, for example as fine-grained igneous rocks, or alternatively as iron-oxide-cemented fine grained sedimentary rocks (e.g. Jake Matijevic, sols 46 and 47; Et Then, sols 86 and 90; Secure, sol 560) [Stolper *et al.*, 2013; Blaney *et al.*, 2014] and accordingly, some caution is warranted in discussing these rocks.

*Possible Igneous* (n = 4, Figure 4.2f) A small subset of float rocks and a large clast within a conglomerate have relatively dust-free surfaces where we observe interfingering light and dark patches whose color does not relate to grain boundaries, but instead creates (in some examples) a porphyritic texture suggestive of igneous diorites (e.g. Clinton, sol 512; Ruker, sol 387; Reedy, sol 526). These rocks are categorized as possible igneous because we see some igneous texture, but we cannot exclude the possibility that the sample is sedimentary and composed of cemented igneous phenocrysts.

*Diagenetic.* (n = 38, Figure 4.2g) A variety of diagenetic features have been identified during the traverse, including nodular concretions [Stack *et al.*, 2014], raised ridges [Siebach *et al.*, 2014], light-toned veins [Nachon *et al.*, 2014], and dendritic concretions [Grotzinger *et al.*, 2015; Kah *et al.*, 2015]. Targets on these features that are clearly related to diagenetic fluids and preferential or replacement cementation are categorized as diagenetic targets. Diagenetic targets do not fit the assumption of only closed-system weathering, so these targets are not used to constrain source rock chemistry.

*Murray Mudstone* (n = 27, Figure 4.2h) On sol 750, *Curiosity* crossed the boundary between Bradbury group alluvial fan and delta deposits, derived from the northern rim of Gale, and the lacustrine mudstones of the Murray formation, the stratigraphically lowest unit of the Mount Sharp group [Grotzinger *et al.*, 2015]. As a lake deposit the mudstone may be derived from multiple sources, given that slopes transporting sediment dip from all directions toward the northern crater moat where the Murray mudstone accumulated. We include samples of the Murray formation exposed at Pahrump Hills (up to sol 860) for comparison to the Bradbury group rocks that compose the other 7 categories. The Murray formation at Pahrump Hills is interpreted to be a mudstone because of its fine grain size,

below the limit of resolution. It is interpreted as a lake deposit due to its fine grain size, its laterally continuous millimeter-scale lamination, and its paleogeographic position downslope of delta deposits [Grotzinger *et al.*, 2015]. Locally, the laminated mudstones are overprinted by diagenetic concretions and secondary crystals interpreted as evaporite mineral molds [Grotzinger *et al.*, 2015; Kah *et al.*, 2015].

#### 4.4.2 APXS Compositional Trends with Texture

In order to test whether sample composition varies systematically with grain size, the textural categories defined in the last section were arranged in order of increasing grain size as much as possible. The Murray mudstone (Mount Sharp group) and Sheepbed mudstone (Bradbury group) make up the finest grained endmembers, then the categories for which grain size is measureable follow in order of increasing grain size: fine sandstone, sandstone, and conglomerate. Diagenetic samples were excluded from this analysis. However, uncertain and possible igneous, were included as coarse grained endmembers because texturally, the uncertain category frequently looks most similar to the conglomerates category despite the lack of distinguishable grains, and the possible igneous category includes samples that represent large clasts within conglomerates, which by definition are the coarsest grains. This ordering also parallels and enhances the compositional trends, as shown in Figure 4.3, although the trends are visible even when these categories are excluded because of their lack of measureable grains.

Figure 4.3 shows that the elemental abundances measured by APXS vary systematically with the grain size, or textural category, of the Bradbury rocks.  $\text{SiO}_2$  (Figure 4.3a),  $\text{Al}_2\text{O}_3$  (Figure 4.3c), and  $\text{Na}_2\text{O}$  (Figure 4.3e) are most enriched in the coarsest grained textural categories, whereas  $\text{FeO}_T$  (Figure 4.3b),  $\text{MgO}$  (Figure 4.3d), and  $\text{TiO}_2$  (Figure 4.3f) are most enriched in the finest grained textural categories. Likewise,  $\text{Cr}_2\text{O}_3$ ,  $\text{MnO}$ ,  $\text{Ni}$ , and (less clearly)  $\text{Zn}$  and  $\text{Br}$  are enriched in the finest grained textures, whereas  $\text{P}_2\text{O}_5$ ,  $\text{SO}_3$ ,  $\text{CaO}$ ,  $\text{Cl}$ , and  $\text{K}_2\text{O}$  do not show a correlation with grain size. These trends are most clearly defined by the variation between the fine sandstone, sandstone, conglomerates, and uncertain/possible igneous categories. Although it is the finest grain size fraction, the Sheepbed mudstone (red in Figure 4.4) is not always the compositional endmember, which

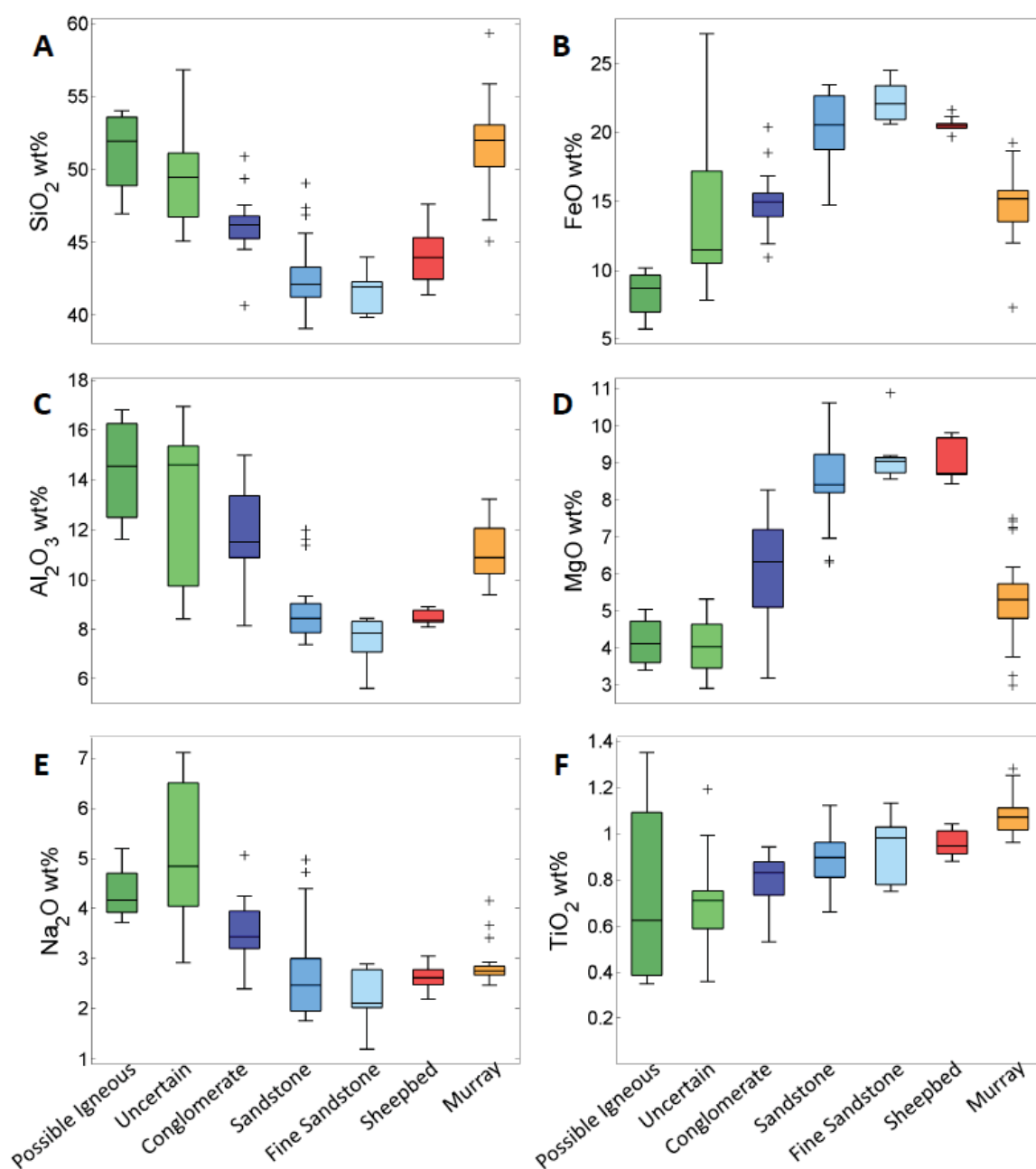


Figure 4.3 Boxplots showing Compositional Differences between Textural Classes  
 Boxplots showing the major elemental compositions of each of the textural classes of Bradbury group rocks ordered from coarsest grained on the left to finest grained on the right in red, and Murray mudstone samples in orange. For each textural group, dark central line represents median data point, colored box encompasses 25<sup>th</sup> and 75<sup>th</sup> percentiles, whiskers typically extend to minimum and maximum data points, but the maximum whisker length is 1.5 times the length of colored box, and crosses demarcate outlier points. Trends show higher concentrations of SiO<sub>2</sub>, Al<sub>2</sub>O<sub>3</sub>, and Na<sub>2</sub>O in coarser-grained textures and higher concentrations of FeO, MgO, and TiO<sub>2</sub> in finer-grained textures.

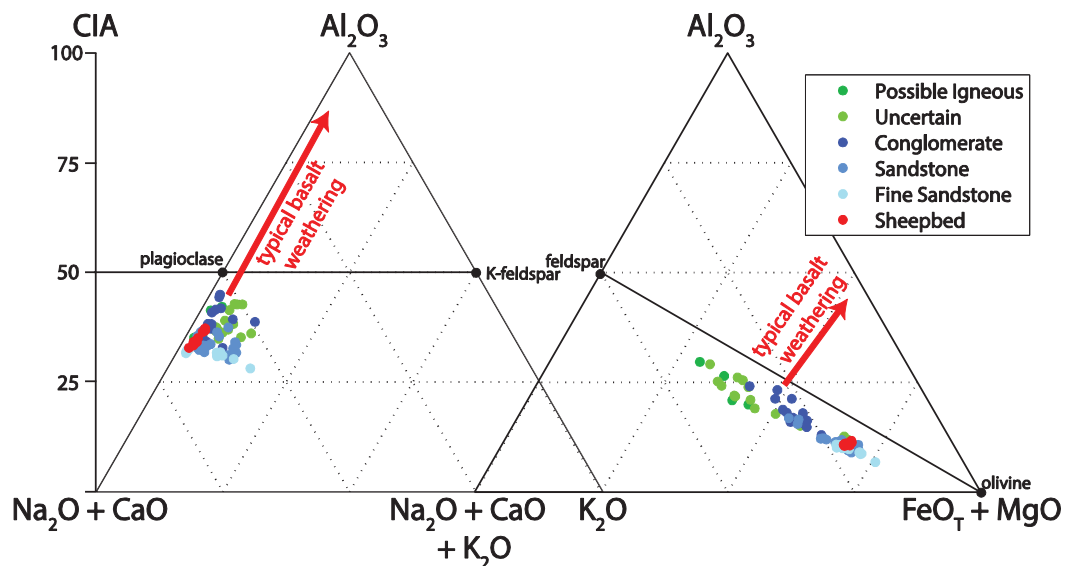


Figure 4.4 Ternary Diagrams for Bradbury Group Textural Classes  $\text{Al}_2\text{O}_3$ - $(\text{CaO} + \text{Na}_2\text{O})$ - $\text{K}_2\text{O}$  (left) and  $\text{Al}_2\text{O}_3$ - $(\text{CaO} + \text{Na}_2\text{O} + \text{K}_2\text{O})$ - $(\text{FeO}_T + \text{MgO})$  (right) ternary diagrams showing the elemental compositions of Bradbury group rocks based on mole fractions. Diagenetic and Murray mudstone textures excluded. Typical terrestrial basaltic weathering trends demarcated with red arrows. Chemical Index of Alteration (CIA) scale, on left, describes molar ratio of labile cations to  $\text{Al}_2\text{O}_3$  content and is a measure of feldspar weathering.

is consistent with the mudstone being a lake sediment that is more likely to accumulate detrital inputs from multiple sources, instead of only the source region for the larger-grained fluvial sediments. The uncertain category frequently has a wider range of compositions than the other categories, as these incorporate float rocks that may not all be part of the Bradbury group depositional system.

To first order, for the Bradbury group, these results indicate that the chemical components of felsic minerals ( $\text{Al}_2\text{O}_3$ ,  $\text{SiO}_2$ , and  $\text{Na}_2\text{O}$ ) are concentrated in the coarsest-grained fraction of the sedimentary rocks, and the chemical components of mafic minerals ( $\text{FeO}_T$ ,  $\text{MgO}$ ,  $\text{TiO}_2$ ,  $\text{Cr}_2\text{O}_3$ ,  $\text{MnO}$ ,  $\text{Ni}$ ) are being concentrated in the finest grained fraction of the sedimentary rocks. These trends describe much of the compositional variability in the Bradbury group rocks, as shown in A-CN-K and A-CNK-FM ternary diagrams in Figure 4.4. Most of the compositional variability between samples is along the feldspar-FM join in the mafic ternary plot and correlated with the sample textures, indicating a distribution between mafic minerals and feldspars, but there is no evidence for significant cation-exchange weathering, which would drive the trends in the direction of the red arrows on Figure 4.4.

This result clearly indicates that composition is related to grain size in the Bradbury group. Assuming negligible chemical weathering, this result could be explained by physical breakdown and transport processes segregating mineral grains, two distinctive source rocks contributing different grain sizes, or a combination of the two. The next several sections describe a series of tests designed to investigate how well these different models explain the spread in the data by first considering why  $\text{K}_2\text{O}$  does not trend with texture, and then testing:

(1) Does the compositional data fit a basic geochemical mixing model for sorting of plagioclase grains from average Mars crustal composition?

(2) Does the compositional data follow igneous differentiation trends from the liquid line of descent of a similar alkali ocean island basalt sequence on Earth?

(3) Does a model that estimates reasonable mineral compositions from the APXS compositional datasets indicate that the rocks could all be consistent with an igneous provenance?

#### 4.4.3 Potassium vs. Stratigraphic Elevation

Potassium is an incompatible element in igneous systems, and therefore makes a good tracer for distinctive igneous sources [Gast, 1968; Engel *et al.*, 1974], especially for sources that have experienced minimal degrees of weathering [e.g. Nesbitt and Young, 1984]. It is particularly interesting in the Bradbury group because it does not trend with texture like the other felsic mineral components ( $\text{Al}_2\text{O}_3$ ,  $\text{SiO}_2$ , and  $\text{Na}_2\text{O}$ ), and instead  $\text{K}_2\text{O}$  appears to be highly concentrated at up to 4% in a few stratigraphic intervals, whereas average Mars crust is 0.45% [Taylor and McLennan, 2009]. Across the 9 km traverse in Aeolus Palus, the sedimentary layers are extremely flat-lying, with measured dips of 0 to +/-3 degrees [Grotzinger *et al.*, 2015], so elevation is used as a simple proxy for stratigraphic layer in Figure 4.5. This shows that the  $\text{K}_2\text{O}/\text{Na}_2\text{O}$  ratio shifts from a steady average of 0.5 to up to 2.5 in samples measured around -4480 elevation, including the Kimberley outcrop. The high potassium (2+ wt%) is found in targets in all of the textural categories that were sampled near that elevation, including fine sandstone, sandstone, conglomerate, and uncertain, but there are no clear textural correlations with potassium within those elevations (such trends may exist, but in this case would likely be obscured by limited sampling, dust cover and/or sampling bias within the relevant elevations). The Windjana sample, a fine sandstone drilled at that outcrop, contains 21% potassium feldspar by weight based on CheMin x-ray diffraction data [Treiman *et al.*, 2015]. This work indicates that a distinctive source of potassium-rich sediments contributed to the Kimberley formation, located within the middle of the Bradbury group [Treiman *et al.*, 2015]. While the source of the potassium is worthy of discussion, the consistent  $\text{K}_2\text{O}/\text{Na}_2\text{O}$  ratio throughout the rest of the Bradbury group shows that whatever the source of potassium here, it does not explain the other major compositional trends.

#### 4.4.4 Modeling trends as a two-component mixture

In order to test the hypothesis that the variability expressed in Bradbury group compositional data can be accurately described as the separation of coarser-grained plagioclase from the finer-grained mafic portion of a relatively typical martian basalt, we use a two-component mixing model [Langmuir *et al.*, 1978]. The model shows the

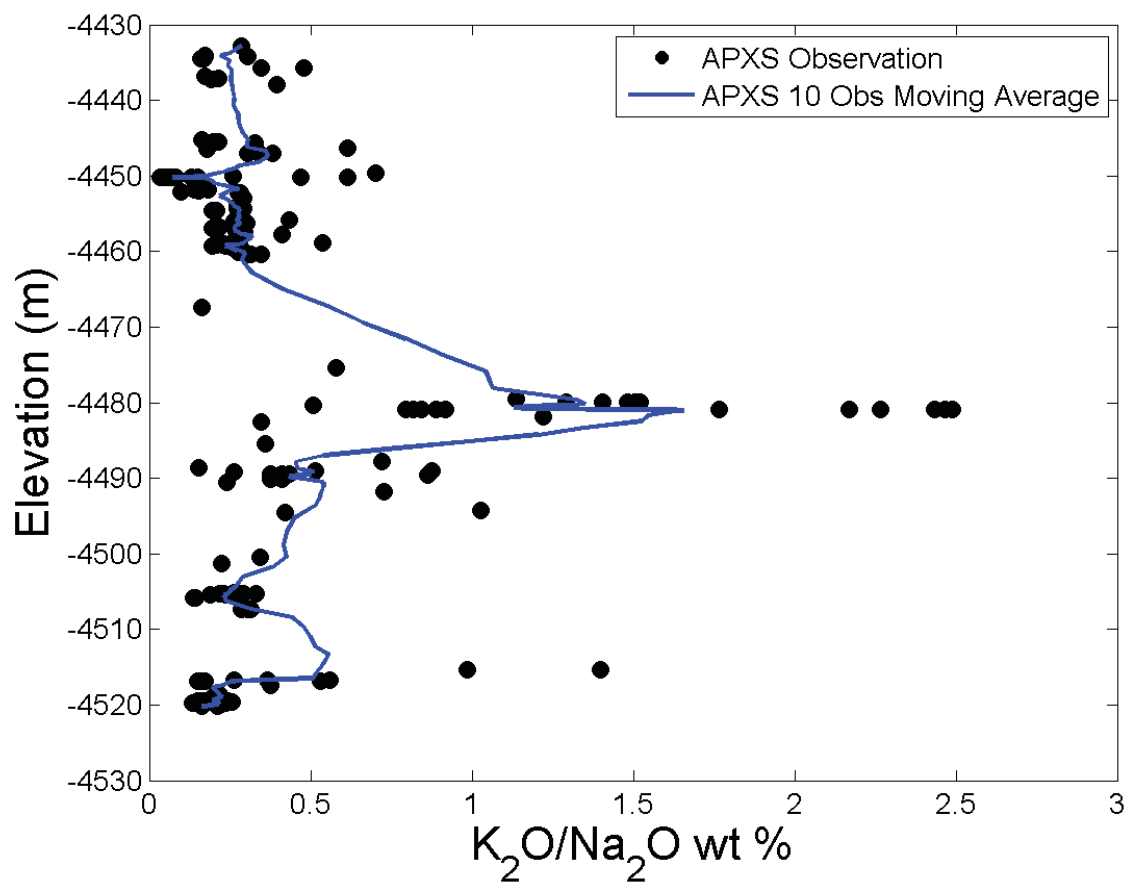


Figure 4.5 K<sub>2</sub>O/Na<sub>2</sub>O vs. Elevation in Samples to Sol 860  
Plot of K<sub>2</sub>O/Na<sub>2</sub>O ratio vs. elevation for each APXS rock sample (excluding diagenetic, but including float rocks). Blue line is 10-point moving average with elevation.

expected trend of average Mars crust basalt plus-or-minus normative plagioclase, which can then be compared to the trend and spread of the APXS dataset. The advantage of using a two-component mixing model is that it is a hypothesis-driven approach to testing when the dataset does or does not fall along the model for each element-element plots. Deviations from the model can then be explained.

#### 4.4.4.1 Methods

Average Mars crust was defined as the starting point for the two-component mixing model because it provides a comparison to other Martian datasets [*Taylor and McLennan, 2009*]. Although the measurements at Gale indicate that the local Noachian crust is more alkaline and mafic than average Mars crust [*Stolper et al., 2013; McLennan et al., 2014; Treiman et al., 2015*], those compositional differences are relatively small and will be reflected as offsets from the model, which can be easily identified. The felsic endmember for the model is the CIPW normative plagioclase based on the average Mars crust composition, An40. This is quite close to the An36 measured by CheMin for the Sheepbed mudstone [*Morrison et al., 2015*], so it provides a good starting plagioclase endmember value. Any deviation from this value would result in a change in the angle of the trend created by the measured sediments relative to the angle expected for an element-element plot based on the model. The overall two-component mixing model, shown for FeO vs SiO<sub>2</sub> in Figure 4.6a, therefore simply represents a line between the composition of plagioclase An40 and the mafic component of average Mars crust, or the composition of Average Mars crust minus the composition of An40 plagioclase.

The presence of variable dust cover on the observed APXS samples presents a complication for the two-component mixing model. The precise composition of the dust is unknown, and there are very few brushed samples to compare with unbrushed samples to obtain a robust estimate for dust composition. A common solution is to use the wt% of SO<sub>3</sub> + Cl as a proxy for dust and soil cover for each sample, and to divide those two components out and renormalize all other elements to 100 wt% [*Rieder et al., 1997*]. This approach assumes that there is negligible SO<sub>3</sub> or Cl in the rocks themselves, and that the dust contains no other significant elements, which may be poor assumptions here. In order to use this

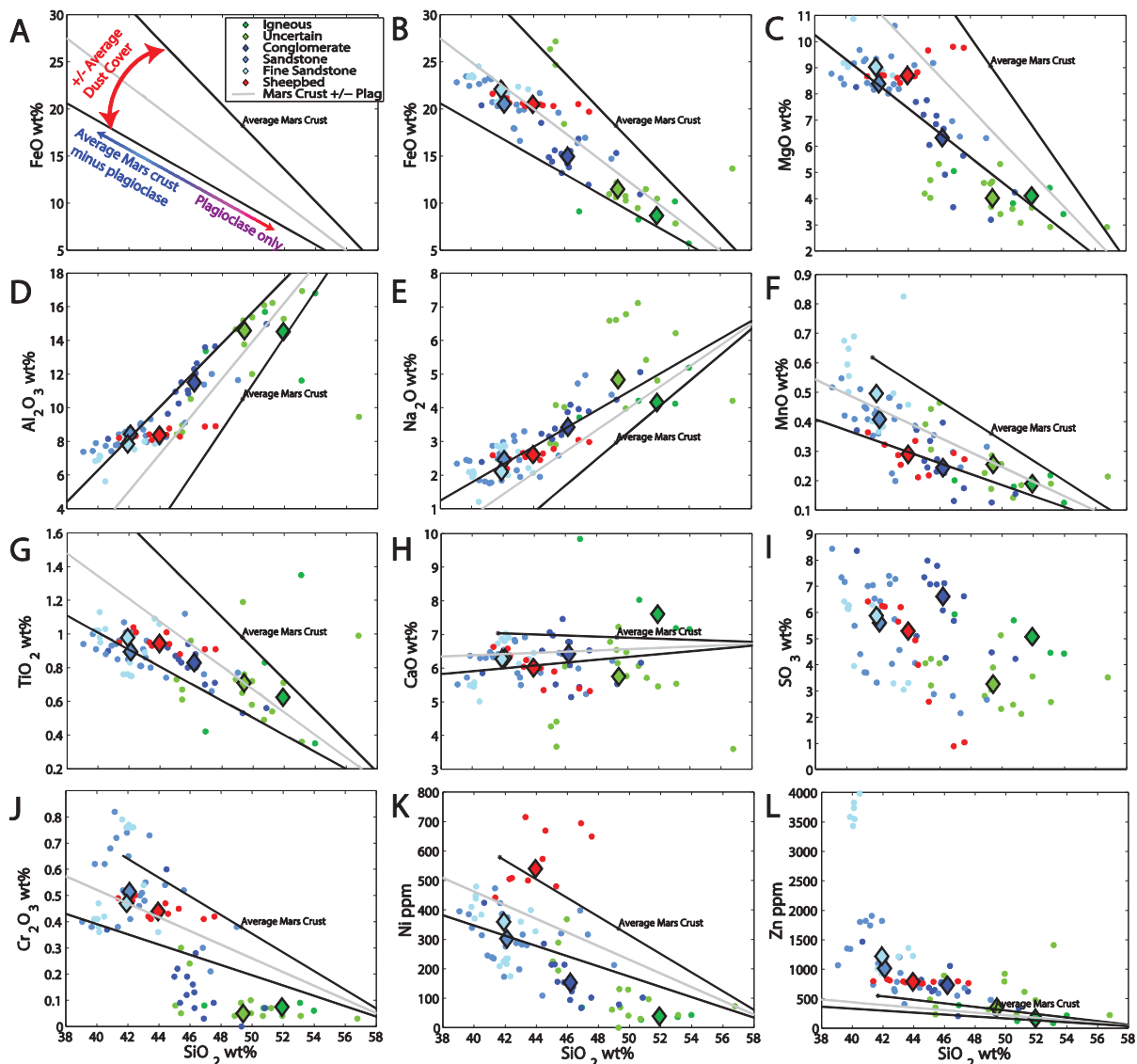


Figure 4.6 Two-Component Geochemical Model for Plagioclase Addition/Subtraction  
 Element-SiO<sub>2</sub> plots showing Bradbury group compositional data compared with two-component geochemical model for segregation of average Mars crust normative plagioclase (An<sub>40</sub>), high SiO<sub>2</sub>, marked in red in part (a), from the mafic components of average Mars crust, low SiO<sub>2</sub>, marked in blue in part (a). Grey line shows geochemical model for average dust cover, black lines represent envelope between no dust cover (marked with average Mars crust composition), and 2x average dust cover. Colored points represent APXS samples, excluding diagenetic samples. Diamonds are median values for each textural group.

approach but avoid assumptions about the dust composition, we use the average concentration of  $\text{SO}_3 + \text{Cl}$  for all included samples (6.1 wt%) as an acceptable error window around the predicted model composition. Since the reported average Mars crust values include no  $\text{SO}_3$  or Cl, we dilute the average Mars crust model by 6.1% to obtain expected model values for analyses with average dust cover. We then present the model with an acceptable error window, bracketing the expected model values (with average dust cover, or a 6.1% dilution factor) with lines that represent average Mars crust (0% dust cover) and twice the average dust cover (a 12.2% dilution factor) (Figure 4.6a).

#### 4.4.4.2 Results

Several of the element-element plots with modeled mixing lines and APXS data are shown in Figure 4.6. For most major elements in Bradbury group samples, compositional variation trends are consistent with the modeled trend of addition or subtraction of plagioclase. Furthermore, the variation along this plagioclase addition/subtraction trend parallels the differentiation between samples by grain size, suggesting again that this primary axis of compositional variation is coupled with sediment grain size.

The two-component model is a forward model with built-in assumptions, so minor differences between the model and the plotted samples are expected. Data variability within the black lines designed to show the range of 0-2x average dust cover is assumed to be primarily due to variations in dust cover. Further scatter may be due to minor or local secondary processes. Beyond scatter, there are three main types of differences between sample compositions and the model based on average Mars crust: (1) offsets related to differences between average Gale Crust and average Mars crust, (2) angular differences between the trend from the samples and the model prediction related to differences between samples that are not captured by An40 plagioclase addition/subtraction, and (3) data clouds instead of trends for elements whose distribution is unrelated to grain size or plagioclase variations. That is, only elements previously identified as having no compositional trend with grain size (Figure 4.3) fall into this category, including  $\text{P}_2\text{O}_5$ ,  $\text{SO}_3$  (Figure 4.6i), CaO (Figure 4.6h), Cl, and  $\text{K}_2\text{O}$ .

Offsets between the modeled composition based on average Mars crust and the typical Bradbury compositions occur for certain elements, indicating that the average basaltic crust composition around Gale Crater is different from the predicted average Mars Crust. For major elements, SiO<sub>2</sub> (Figure 4.6) and MgO (Figure 4.6c) in Gale are slightly lower than average Mars crust, and FeO<sub>T</sub> is slightly elevated above crustal values (Figure 4.6b). K<sub>2</sub>O and Zn (Figure 4.6l) are significantly elevated above Mars crustal values in nearly all Bradbury samples. This is consistent with observations made for the Yellowknife Bay formation [McLennan *et al.*, 2014] that indicate that the crust around Gale is more mafic than average crust.

Angular offsets between modeled plagioclase addition/subtraction and the dataset trends show where there are additional factors affecting the data that are not accounted for in the model. The largest angular offsets are in Cr<sub>2</sub>O<sub>3</sub>, Ni, and Zn (Figure 4.6j, k, and l), all of which are more strongly correlated with grain size than the model predicts. These three elements are highly concentrated in the finest grain sized samples such that their concentrations dramatically drop off with increasing grain size, and are especially low in rocks in the uncertain and possible igneous categories (Figure 4.6j, k, and l). In the other direction, TiO<sub>2</sub> and Al<sub>2</sub>O<sub>3</sub> are slightly less strongly correlated with grain size than the model predicts, creating much smaller angular discordances (Figure 4.6d, g). These will need to be accounted for in an overall model of the system.

#### 4.4.5 Comparison with Igneous Evolution Trends

One of the hypotheses for explaining compositional, and likely mineralogical, variation with grain size would be that the more felsic grains come from a different igneous flow than the more mafic grains, implying the presence of magmatic compositions equivalent to or more extreme than the observed endmember rock compositions. In this scenario we must assume that more felsic igneous rocks exist in the same watershed and in close spatial association with the more mafic rocks since both would need to contribute detritus to the same sedimentary rocks. While the two rock types are not required to be genetically linked, it is simplest to initially assume that the initial regional magmatic composition is the same and the different rock types represent different compositional

states of that magma as it cools down a liquid line of descent. In this case, we would likely observe mixed detrital sediments from igneous rocks representing a series of intermediate compositions following the liquid line of descent of the magma. In order to test the similarity of the compositional trends measured in the Bradbury group to the trends produced during cooling of magma along the liquid line of descent, we plot the Bradbury trends (excluding Murray formation and diagenetic samples) against compositional data from igneous samples in the Tenerife alkaline ocean island basaltic sequence (Figure 4.7). Major elements are plotted against MgO content because the amount of MgO is related to the evolution of the basalt from the initial magma.

It is important to recognize that Figure 4.7 compares igneous rocks with sedimentary rocks inferred to be derived from igneous rocks, and is not designed to be a direct comparison of igneous evolution pathways. The goal here is rather to understand how the compositional trends in the Gale Crater dataset compare with igneous differentiation trends for similar bulk basaltic compositions. In that regard, Tenerife ocean island basalts were selected as a compositional analog because they have been previously compared to Gale rocks [Stolper *et al.*, 2013], they have compositions similar to those rocks in the uncertain category, and because the compositions for ocean island basalts are less likely to be complicated by continental surface processes [Sarbas and Nohl, 2008]. Naturally, the magmatic composition on Mars is not exactly the same as the magma composition in Tenerife (e.g. Fe is higher in martian magmas, as shown in Figure 4.7b, and  $\text{TiO}_2$  is lower in Martian magmas, shown in Figure 4.7g [Stolper *et al.*, 2013]), but the minerals formed during cooling and the shapes of the compositional curves would likely be similar if the compositional variation is directly related to magmatic evolution.

Observing the igneous evolution plots in Figure 4.7, it is apparent that the elemental trends in the Bradbury samples are quite linear in comparison with the igneous evolution trends. Linear trends are expected on element-element plots when two-component mixing is taking place, e.g. mixing two sources or physically adding/subtracting a mineral, but elemental trends during igneous evolution of a magma typically show multiple slopes because the ratios of elements being incorporated into solid minerals change during cooling

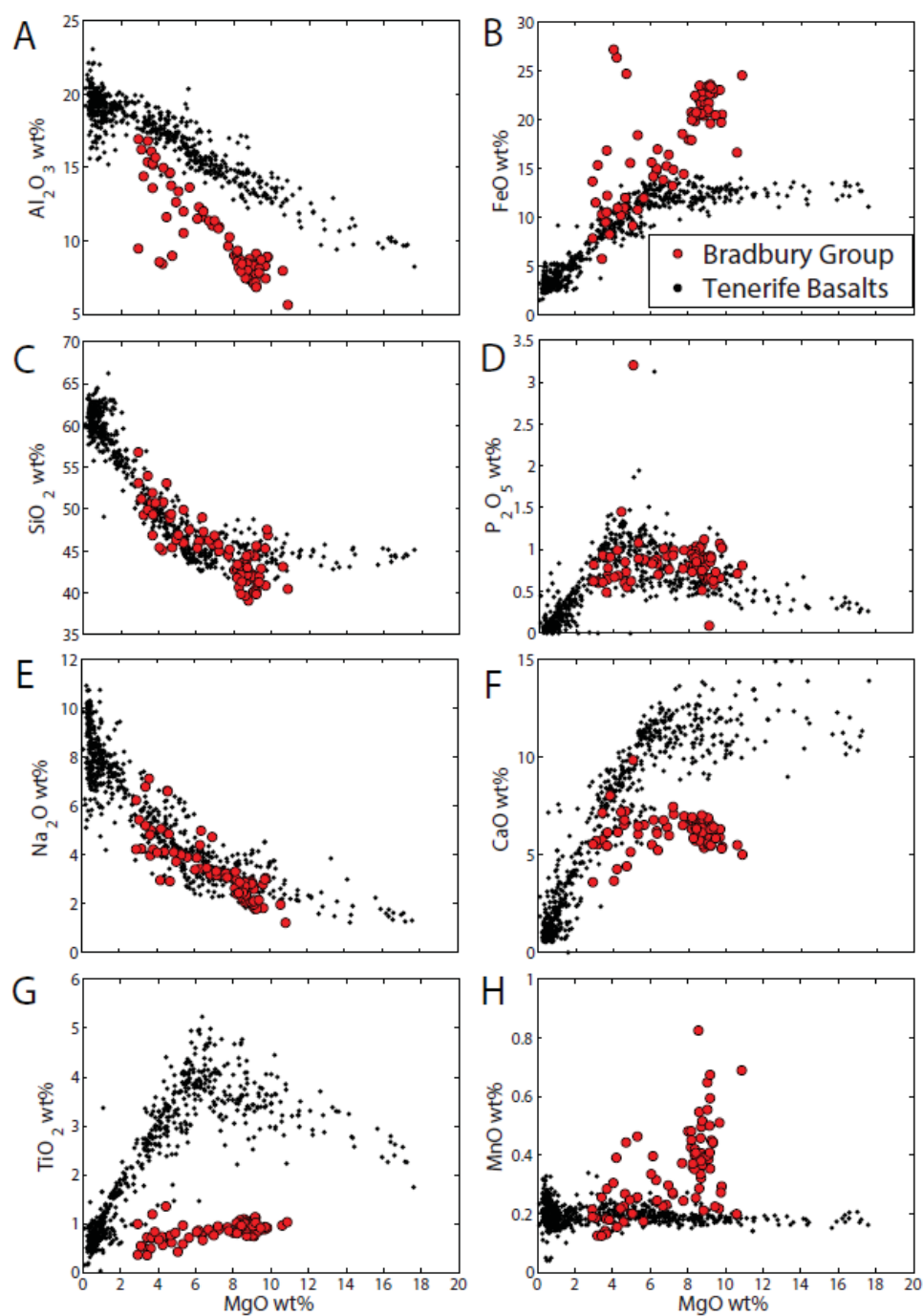


Figure 4.7 MgO Plots Comparing Bradbury Group and Tenerife Ocean Island Basalt Compositions

Element-MgO plots comparing Bradbury group compositional data in red (excludes diagenetic and Murray samples) with Tenerife Ocean Island Basalt compositional data in black. MgO wt% is proportional to magmatic evolution in igneous systems, so for Tenerife basalts, high-MgO samples are primitive and low MgO samples are from more evolved magmas.

as different minerals are formed. So linear trends would be unexpected from igneous evolution processes alone.

The  $\text{Al}_2\text{O}_3$  vs MgO plot in Figure 4.7a is notable because the Tenerife data has the highest slope in  $\text{Al}_2\text{O}_3$  vs MgO of any of the catalogued ocean island basalt complexes [Sarbas and Nohl, 2008] and the slope of the Bradbury trend is significantly steeper. This phenomenon is also present in the MnO vs MgO plot (Figure 4.7h); in magmatic systems, MnO is incorporated into minerals at a near-constant rate, but there is a significant slope between MnO and MgO in the Bradbury group samples, indicating that most of the variation is due to some other phenomenon. These unexpectedly steep slopes make it unlikely that the Bradbury elemental trends are defined by changes in the composition of igneous detritus due to magmatic evolution of the source rocks in the watershed. This does not rule out some igneous evolution for rocks in the watershed of the northern crater wall and rim, but these basaltic provenance shifts must fit within the observed elemental trends, and are unlikely to define them. This also cannot rule out the presence of non-genetically-related, cross-cutting, igneous associations.

#### *4.4.6 Modeling APXS Mineralogy*

Typically, terrestrial rock samples are characterized by a combination of their mineralogy and bulk chemistry, but due to sampling limitations with the rover (in Aeolus Palus, we have bulk compositions of 73 distinct in-situ rocks using APXS and the mineralogy of only 3 samples using the CheMin X-Ray Diffraction instrument), bulk chemistry is the only available information for the majority of these samples. Mineralogy can only be derived from chemistry if a number of assumptions are made, both with respect to the number of minerals included and the specific mineral compositions, e.g. the Fo number for olivine. The most typical of these would be to assume the rock is igneous, and that all minerals in the rock were formed in thermodynamic equilibrium, which would allow a normative mineralogy calculation of the mineral components. The Aeolus Palus rocks are sedimentary, and therefore do not fit those assumptions— instead, they likely include detritus derived from a range of basaltic sources that is sorted during transport, and may include cement compositions precipitated under different aqueous geochemical

regimes. However, as shown in Figure 4.3, the bulk chemistry of the Aeolus Palus samples appears consistent with only cation-conservative weathering of basalt, so if that is correct, the compositions could potentially be related to primary igneous minerals.

#### 4.6.1 Methods

In order to estimate the mineralogy of the Bradbury rock compositions and test the assumption of minimal open-system chemical weathering for those samples that do not show visible evidence of diagenetic overprinting, we use a Monte-Carlo based mass-balance model to test whether the rock compositions as determined by APXS are consistent with a mixture of primary igneous minerals whose compositions are, in turn, constrained by the compositions of phases in martian meteorites [e.g. *Papike et al.*, 2009; *Gross et al.*, 2011; *Santos et al.*, 2015; *Wittmann et al.*, 2015] and by the analysis of CheMin data on three Gale Crater samples [*Vaniman et al.*, 2014; *Morrison et al.*, 2015; *Treiman et al.*, 2015]. The minerals included in the calculations are: olivine, high- and low-Ca pyroxene, plagioclase, K-feldspar, apatite, ilmenite, chromite, iron oxides, and silica and the mass balance calculation attempts to find the best set of phase proportions in a least-squares sense that minimizes deviations between the calculated bulk composition and the measured bulk composition for the following oxides: SiO<sub>2</sub>, TiO<sub>2</sub>, Al<sub>2</sub>O<sub>3</sub>, Cr<sub>2</sub>O<sub>3</sub>, FeO, MnO, MgO, CaO, Na<sub>2</sub>O, K<sub>2</sub>O, P<sub>2</sub>O<sub>5</sub>, and NiO. While mass balance calculations are widely used in petrology [e.g. *Bryan et al.*, 1969; *Reid et al.*, 1973; *Walter et al.*, 1995], their application to the mixing problem discussed here is complicated by the fact that we have very limited information on the compositions of the major phases [*Vaniman et al.*, 2014; *Morrison et al.*, 2015; *Treiman et al.*, 2015]. However, using the compositions of mineral phases in martian meteorites and mineral stoichiometric constraints [see *Baker and Beckett*, 1999], we can construct, using random numbers, a population of stoichiometric olivines, pyroxenes, plagioclases, etc., whose compositions are consistent with those of martian meteorites, and, pulling phase compositions from these populations, run a very large number of mass balance calculations for each sample. In constructing these phase compositions, cation abundances in the olivines (Cr, Mn, Ca, and Ni) and pyroxenes (Ti, Al, Cr, Mn, Ca, Na,

and Ni) were related to Mg# [ $\text{Mg}/(\text{Mg} + \text{Fe})$ , molar] variations in each phase and the bounds on Mg# of olivine and pyroxene and on molar  $\text{K}/(\text{K} + \text{Na})$  of the alkali feldspar (which defines its composition) were constrained by CheMin results; bounds on molar  $\text{Ca}/(\text{Ca} + \text{Na})$  values in plagioclase were based on data from martian meteorites and CheMin. It is important to note that although each individual mass balance calculation is over-determined (i.e., there are more equations than unknowns), the Mg# bounds on the olivine and pyroxenes are relatively loose and bulk FeO and MgO exert the largest constraints on the calculated proportions of mafic phases; hence, the individual weight fractions of these three phases are not as well constrained as their sum. We also note that the alkaline nature of many of the rocks at Gale Crater [e.g. *Stolper et al.*, 2013; *Schmidt et al.*, 2014; *Sautter et al.*, 2015] suggests that the pyroxenes in these rocks may differ from those found in martian meteorites (pyroxenes in terrestrial alkaline rocks tend to be richer in Ti, Al, and Na compared to pyroxenes in tholeiites). However, as we show below, the majority of the mass balance calculations yielded extremely small residuals, indicating that martian meteorite phase compositions can successfully be used to mass balance the compositions of Gale Crater sedimentary rocks.

In the calculations presented here, 200,000 weighted mass-balance runs were done for each sample—the best-fit calculation for any sample was that run with the lowest  $\chi^2$  value. Each best-fit calculation for a given sample was only deemed statistically acceptable if the  $Q$ -value [e.g. *Press et al.*, 1992] for that run was  $\geq 0.05$  (i.e., acceptable at the 95% confidence level). Note that the low-Ca pyroxene in our calculations was pigeonite. Based on Rietveld refinements of CheMin data [*Vaniman et al.*, 2014; *Morrison et al.*, 2015; *Treiman et al.*, 2015], pigeonite appears to be substantially more abundant than orthopyroxene in Gale Crater rocks and including three pyroxenes in the mass balance calculations leads to a linear degeneracy. Nevertheless, even with only two pyroxenes, some mass balance calculations returned negative mass fractions of olivine and/or pyroxene; after every individual calculation in a set of 200,000, any negative coefficients were set to zero and the mass balance calculation was repeated using the same phase compositions. As noted above, bulk APXS compositions were renormalized on a S- and Cl-free basis. Although this may introduce a systematic bias (we discussed

above why we think that such a bias, if it exists, would not be large), initial calculations that included anhydrite and halite resulted in best-fit plagioclase compositions that tended to be extremely albitic, i.e., with molar  $\text{Ca}/(\text{Ca}+\text{Na})$  ratios of 0.1 to 0.2—substantially more sodic than plagioclase compositions estimated by CheMin [Vaniman *et al.*, 2014; Morrison *et al.*, 2015; Treiman *et al.*, 2015]. This suggests that although CaO and  $\text{SO}_3$  are positively correlated in the APXS data, some fraction of the sulfur is incorporated in non-calcium bearing phases. The fact that we have only mass-balanced rocks that show no obvious diagenetic features (and have  $\text{SO}_3$  contents rocks  $<8.4$  wt%) limits the leverage that the renormalization exerts on the remaining oxides in these bulk compositions. Details of the mineral calculation schemes and the mass balance program will be presented in a subsequent paper.

Although a large majority of the APXS sedimentary rock compositions can be modeled using only the compositions of igneous minerals that are consistent with those found in martian samples, this does not mean that these sedimentary rocks are necessarily composed of just these phases. Indeed, based on the results of the small number of CheMin XRD analyses, there may well be clay minerals and one or more difficult-to-characterize amorphous phases in all of the Gale Crater sedimentary rocks [Vaniman *et al.*, 2014; Treiman *et al.*, 2015]. It does suggest, however, that the compositions of the materials that accumulated to produce these sedimentary rocks can be described as mixtures of igneous minerals and that a substantial loss of cations following deposition has probably not occurred. Calculations using bulk compositions of progressively more severely weathered basaltic rocks [Chesworth *et al.*, 1981; Nesbitt and Wilson, 1992; Sheldon, 2003] show that mass balance fits generally fail at the 95% confidence level once the Chemical Index of Alteration (discussed in section 4.5.1) exceeds  $\sim 50$ – $55$ . Furthermore, if a significant number of the observed samples can be mass balanced using a relatively narrow range of olivine, pyroxene, and feldspar compositions, then that would suggest that the sources of these sedimentary rocks consisted of igneous rocks with a fairly limited range of compositions and that only physical weathering and sorting operated to produce the observed elemental trends. An important caveat on this last point is that the phase compositions used in the mass balance calculations should be thought of

as average compositions, i.e., a relatively wide range of plagioclase compositions could actually be present in the sedimentary rock but the best-fit plagioclase from the mass balance calculation would be one that closely matched the average composition of all of the plagioclase grains.

#### 4.6.2 Results

Seventy-four out of eighty-three non-diagenetic rock analyses, or about 90% of the non-diagenetic Bradbury group analyses, were successfully modeled as sums of primary igneous minerals with a  $\chi^2$  confidence interval of 95%. This is consistent with the assumption of cation-conservative weathering (Figure 4.3) [McLennan *et al.*, 2014], and further confirms those results by showing that all of the elements that are measured with APXS can be reasonably arranged in primary igneous compositions within most of these rocks, with no need for any cation loss to explain the compositions. This does not preclude the formation of secondary minerals—indeed, we know that secondary minerals are included—but the compositions are consistent with cation-conservative authigenesis rather than open-system weathering.

Of the nine Bradbury group analyses that could not be modeled at 95% confidence, four were consistent within the 80% confidence interval and had one element that could not quite be incorporated into the primary basaltic minerals, including Jake\_Matijevic2 (sol 47, uncertain, excess Na<sub>2</sub>O), Stirling (sol 707, sandstone, excess Na<sub>2</sub>O), JumJum (sol 550, conglomerate, excess Na<sub>2</sub>O), and Windjana DRT (sol 612, fine sandstone, excess MnO). The other five were all float rocks that were categorized in the “uncertain” category, and all five cases had excess Na<sub>2</sub>O. These include two analyses on Jake\_Matijevic1 (sols 46 and 47, excess SiO<sub>2</sub> and Na<sub>2</sub>O), Oscar (sol 516, excess Na<sub>2</sub>O and Al<sub>2</sub>O<sub>3</sub>), Morehouse (sol 503, excess Na<sub>2</sub>O and SiO<sub>2</sub>), and Secure (sol 560, excess Na<sub>2</sub>O and Al<sub>2</sub>O<sub>3</sub>).

Only 26 of 38 of the diagenetic and 16 of 27 Murray mudstone samples had  $\chi^2$  values indicating fit at 95% confidence, indicating that the composition of these subgroups has been affected by chemical weathering, chemical addition, and/or chemical alteration. Diagenetic samples were categorized as such because they contain textural features showing preferential cementation, so it is interesting that ~70% of them can still be

modeled with primary igneous components, however it is important to note that this model is done on a volatile-free basis, so, e.g., excess  $\text{CaSO}_4$  cement or vein-fill may not be captured by this model. The Murray mudstone samples could only be modeled with a silica mineral component, and frequently had excess  $\text{Al}_2\text{O}_3$ ,  $\text{Na}_2\text{O}$ , and/or  $\text{P}_2\text{O}_5$  compared to the closest primary basaltic mineral composition. This is consistent with previously published reports showing that the Murray mudstone sediments have been more affected by some form of chemical weathering [McLennan *et al.*, 2015].

The mineralogical models for the Bradbury group APXS compositions allow mineral-based comparisons between the different textural classes. A bar chart showing the median modeled mineralogy of each textural class is shown in Figure 4.8a. This chart is consistent with the geochemical models in Figure 4.6, indicating that the mineralogy, like elemental composition, varies with grain size in for the Bradbury group, and that one of the primary differences with grain size is the weight percent of plagioclase minerals (Figure 4.8b) compared with the weight percent of mafic minerals (Figure 4.8c). Plagioclase content is quite high in possible igneous and uncertain float rocks, intermediate in conglomerates, and lower in sandstone, fine sandstone, and Sheepbed mudstone targets. Mafic mineral content (olivine, high- and low-Ca pyroxene, chromite, ilmenite, and iron oxides) is higher in the three finest grained textural classes.

Other differences between textural classes are irregular. Based on the range of mineral compositions that led to acceptable fits for each composition, the relative amounts of olivine, high-Ca, and low-Ca pyroxene are not well constrained, but the sum of these three components is well constrained, so it may be more accurate to consider the sum of mafic components (Figure 4.8c) rather than the relative proportions of each as shown in Figure 4.8a. From Figure 4.6h, it is evident that calcium content does not trend with grain size and instead has a relatively consistent value in all samples (like sulfur, Figure 4.6i). Calcium sulfate veins are known to pervasively transect every unit *Curiosity* has explored, including the Bradbury group [Nachon *et al.*, 2014], the Murray formation [Grotzinger *et al.*, 2015; Kah *et al.*, 2015; Kroynak *et al.*, 2015] and Stimson formation [Newsom *et al.*, 2016], so it is evident that some calcium was transported in late-stage diagenetic fluids. If

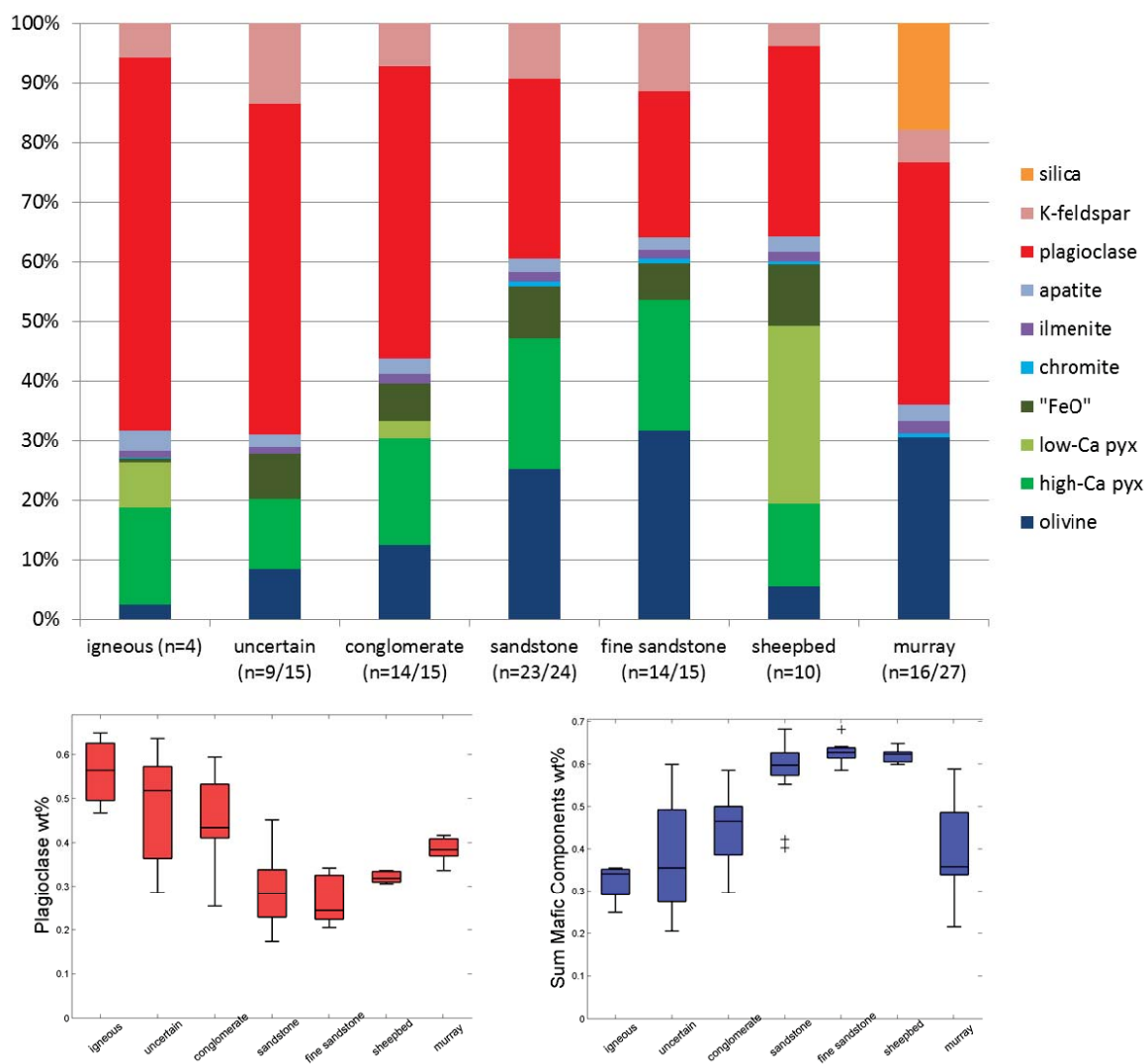


Figure 4.8 Modeled Mineralogy for Each Textural Class in Bradbury Group

Diagrams showing the modeled mineralogy for each of the Bradbury group textural categories and Murray mudstone. Part (a) shows median weight percent of each mineral for each textural class. Parts (b) and (c) are boxplots showing the range of plagioclase and mafic components within the textural classes. Part (c) sum of mafic components is the sum of olivine, pyroxenes, "FeO", chromite, and ilmenite.

calcium has been redistributed by diagenetic fluids, then the relative proportioning of Ca between high and low calcium pyroxene could be further compromised.

## 4.5 Discussion

Any hypothesis for explaining observed APXS compositional variations between Bradbury Group samples must address variation from chemical weathering, source rock input, transport processes, and diagenetic cements. This study has shown that a meaningful hypothesis must also be constrained by these observations:

(1) Compositional variation between non-diagenetic Bradbury samples is nearly linear on element-element plots and is strongly correlated with grain size/texture of the sedimentary rock observed (Figures 4.6 and 4.7).

(2) This compositional variation is consistent with the enrichment (in coarser-grained samples and float rocks) or depletion (in fine-grained rocks) of plagioclase minerals (Figures 4.6 and 4.8).

(3) Bradbury rocks have extremely low Chemical Index of Alteration values (Figure 4.3) and 90% of the sample compositions can be modeled using only primary basaltic minerals (Figure 4.8).

(4) Potassium does not follow expected trends for plagioclase enrichment, and is instead strongly enriched in a specific stratigraphic position (Figure 4.5).

### 4.5.1 Chemical Weathering

Chemical weathering involves the decomposition of rocks by chemical reactions that break apart the constituent minerals, typically forming new secondary minerals. This process can occur in an open system or a closed system. In an open system, some chemical products from mineral and rock breakdown may be removed from the system, typically by dissolution and fluid migration, causing changes in the bulk chemistry of the rock sample. In a closed system, chemical breakdown of the rocks occurs but the chemical constituents remain, forming secondary minerals but not changing the bulk chemistry of the rock. The APXS instrument onboard *Curiosity* only measures bulk composition of rocks, and therefore is only sensitive to chemical weathering in an open system; the formation of

secondary minerals in a closed system does not affect the bulk compositions and is not distinguishable with the APXS instrument alone.

In this study, three methods are used to assess the degree of open-system chemical weathering; Chemical Index of Alteration (CIA) values, trends on the mafic ternary diagram, and mineralogical modeling to see if sample compositions deviate from primary basaltic mineral components. All three methods, described below, indicate that open-system chemical weathering in the Bradbury Group rocks was negligible.

Open-system chemical weathering in ancient rocks on Earth and Mars is frequently quantified using the Chemical Index of Alteration (CIA), a molar ratio of  $\text{Al}_2\text{O}_3$  over the sum of  $\text{K}_2\text{O}$ ,  $\text{CaO}$ ,  $\text{Na}_2\text{O}$  and  $\text{Al}_2\text{O}_3$  that serves as a proxy for the weathering of feldspars and Ca-bearing pyroxene (Figure 4.3) [Nesbitt and Young, 1982; 1984; Nesbitt, 2003; McLennan *et al.*, 2014]. On Earth,  $\text{CaO}^*$  is corrected to only include calcium in silicate minerals; since this is not well-constrained on Mars, we do not apply a correction here, so reported CIA values are lower than they would be if corrected. Fresh mafic basalts have CIA values of ~30-45; values above ~45 may indicate some exposure to weathering, and values above ~50-55 are evidence for some history of open-system chemical weathering [McLennan *et al.*, 2014]. Since the rocks in Aeolus Palus are basaltic, and the first components to chemically weather are likely olivine and any basaltic glass, it is important to also look for weathering trends on the mafic ternary diagram A-CNK-FM, which also incorporates  $\text{FeO}_T$  and  $\text{MgO}$ , so that trends from weathering of olivine would also appear along the direction of the red arrow in Figure 4.3.

The lack of open-system chemical weathering in the Yellowknife Bay formation, the lowest part of the Bradbury group, was first established by detailed measurements of the Sheepbed mudstone. Compositional data for this unit are very similar to average Mars crust [Taylor and McLennan, 2009] and have very low CIA values (up to 37.5), indicating that there was minimal or no open-system chemical weathering of detrital basalt [McLennan *et al.*, 2014]. However, CheMin x-ray diffraction data revealed that this unit is composed of 20-30% phyllosilicates, which are interpreted to be authigenic clays formed within the ancient lake that deposited the mudstone [Grotzinger *et al.*, 2014; Vaniman *et al.*, 2014]. These observations indicate that even where significant amounts of water were

present, authigenesis occurred, and secondary minerals were formed, there is still a lack of evidence for open-system chemical weathering. The lack of evidence for chemical weathering was attributed to a cold climate by McLennan et al. [2014].

Observations of coarser-grained Bradbury sediments also show a lack of evidence for open-system chemical weathering. Of 113 rock targets, 10 have CIA values above 40, and all are below 45. No weathering trends appear on the mafic ternary diagram (Figure 4.3). Additionally, 90% of all of the non-diagenetic rock compositions observed, including float rocks, can be modeled as a mixture of primary basaltic mineral compositions with a 95% confidence interval (Figure 4.8). There is remarkably little evidence for any extensive chemical alteration or cation loss from these sediments. Note that this trend does not continue into Mount Sharp sediments, which show a more complex weathering history, resulting in CIA values of 37-53, with only 4 samples having CIA < 40, and 40% of the samples cannot be modeled by primary basaltic minerals + silica.

Overall, there is a lack of evidence for chemical weathering of Bradbury group sedimentary rocks, indicating that none of these samples has experienced a significant weathering history. We support the original interpretation of this trend by McLennan et al. [2014] who invoked a cold climate at the site of weathering along the crater rim. The climate was warm enough to allow liquid water to be stable and support overland flows [Williams et al., 2013; Grotzinger et al., 2014; Szabo et al., 2015] and also pool as long lived lakes [Grotzinger et al., 2014; Grotzinger et al., 2015]; however, it was cool enough to severely limit the effects of chemical weathering.

#### *4.5.2 Mechanisms for Potassium Variation*

Perhaps the most distinctive elemental trend in the measured suite of Bradbury samples – potassium variation – is not correlated with grain size but is instead strongly correlated with bedrock and float measurements at a certain stratigraphic interval (Figure 4.5). As with other elements, potassium could be enriched by: contribution of a distinctive source region enriched in potassium (as suggested by [Treiman et al., 2015]), hydrodynamic sorting of potassic minerals during transport, or post-depositional chemical

alteration such as potassium metasomatism. Treiman et al. [2015] discuss the source of the potassium in detail; we summarize key relevant arguments here.

Increased potassium due to hydrodynamic sorting of potassium during transport or potassium metasomatism within the sediments in the Kimberley outcrop is inconsistent with the APXS and CheMin observations. Potassium does not trend with grain size, and the presence of easily-altered olivine, pyroxene, and other primary igneous minerals in the drilled (“Windjana”) sample and the lack of any other evidence for open-system chemical alteration are inconsistent with significant chemical weathering. Furthermore, potassium metasomatism is unlikely due to the lack of accompanying metamorphic or hydrothermal alteration minerals [Fedo et al., 1995; Treiman et al., 2015], so the potassium must be concentrated by another mechanism.

The trend in potassium with stratigraphic position (Figure 4.5) makes it clear that potassium is highly concentrated in a specific sedimentary interval, which is likely correlated with detrital input from a high-potassium source rock. There was a drilled sample at the site of the high potassium, “Windjana”, so the CheMin X-Ray Diffraction (XRD) data allows a more detailed analysis of the potassium source [Treiman et al., 2015]. To first order, Windjana XRD results showed that the sample contains significant amounts of pigeonite (11%) and sanidine (21%), which cannot form in the same igneous protolith, so based on mineralogy alone, multiple igneous protoliths must have contributed to this sample.

Investigation of the crystal chemistry of the mineral components based on the XRD analysis reveals further evidence that the potassium source is a distinctive detrital component. Treiman et al. [2015] show that the sanidine is ~Or95, with extremely high  $K_2O/Na_2O$ . This is a surprising finding in Aeolus Palus, where the rest of the plagioclase is andesine (~An30-50) [Vaniman et al., 2014; Morrison et al., 2015]. Treiman et al. also analyze the crystal chemistry of the major basaltic components, and show that the olivine, augite, and pigeonite are consistent with formation in the same basaltic protolith (within error)—although this cannot be the same protolith as the sanidine. The implication is that the majority of the components in the sample are correlated, and from a basaltic source that is likely related to the rest of Aeolus Palus, and Or95 sanidine is the only significant tracer

mineral contributed by a distinctive igneous provenance, which Treiman et al. [2015] interpret to be a trachyte with >40% sanidine. For further details and petrologic implications, we refer the reader to the Treiman et al. [2015] study.

The protolith with the sanidine mineral component was only contributing significant sediment at certain times during the filling of the Gale basin, which caused certain stratigraphic intervals, such as the Kimberley formation, to be strongly enriched in sediment from that source region, whereas other intervals were not affected (Figure 4.5). Without sufficiently high resolution chemostratigraphic data collected across this part of the Bradbury group, it is not clear whether or not hydrodynamic sorting had any effect on potassium distribution within the Kimberley formation.

### *4.5.3 Major Influences on Composition of Bradbury Group*

#### **4.5.3.1 Influence of Source Rocks**

The provenance of sedimentary rocks describes the collection of all rock types that are weathered and eroded to produce sediment that is transported and deposited in a sedimentary basin. Sedimentary provenance studies use the chemical and mineralogical properties of sedimentary rocks to determine the original source rock composition and the effects of weathering processes that caused the source rock to break down into sediment [McLennan et al., 2003; Weltje and von Eynatten, 2004]. For fluvial sediments, source rocks are typically the local rock units upstream in the watershed that are exposed to surface weathering [Nesbitt et al., 1996]. Eolian, volcanoclastic, and lacustrine sediment sources are frequently more widespread because they can integrate rock fragments transported longer distances by wind and sediments from all catchments around the basin. In terrestrial cases, the majority of sediment is derived from pre-existing sediment (i.e. sediment recycling), which obscures identification of original igneous/metamorphic sources. The role of sediment recycling is not well constrained for Mars, but it is not believed to play as significant a role [McLennan and Grotzinger, 2008a].

Provenance studies that correlate sedimentary rocks to their original source rocks typically depend on bulk composition and petrology of the rocks [Russell, 1937; Young and Nesbitt, 1999; Vezzoli et al., 2004], detrital heavy minerals [Frihy, 1994; Cawood et

*al.*, 2003; *Fedo et al.*, 2003], or radiogenic isotope fractionations within minerals [*Vervott et al.*, 1999; *Kuhlmann et al.*, 2004; *Hodges*, 2005] to describe the sediment provenance. The history and background for each of these approaches is summarized in [*Weltje and von Eynatten*, 2004]. While provenance effects can be obscured by sorting of grains during transport and later diagenetic processes, the initial relative sizes of different mineral grains are defined by the source rocks, so the direction of sorting trends depends heavily on provenance [*Ohta*, 2004; *Fedo et al.*, 2015].

The sedimentary materials of the Bradbury group were likely sourced from the Noachian terrain above the northern rim of the crater based on sediment transport directions and local geomorphic and stratigraphic features [*Palucis et al.*, 2014; *Grotzinger et al.*, 2015; *Szabo et al.*, 2015]. Rocks within this region are known from orbital hyperspectral imagery to contain olivine [*Ehlmann and Buz*, 2015], but otherwise there are relatively few constraints on the petrology of the watershed, so we do not know *a-priori* what provenance signals may be expressed in the detritus which accumulated as the Bradbury group. However, from the perspective of the bulk Bradbury composition we gain some insight into the overall nature of the sediment source; the compositions tend to be similar to average Mars crustal basalt, but somewhat more alkaline, comparable to alkaline ocean island basalts on Earth [*Stolper et al.*, 2013].

Direct information about the Gale provenance can also be based on analysis of large grains of definitively igneous rocks. While *Curiosity* has observed several rocks with potentially igneous textures (and observed 4 of these with APXS), the most definitive igneous rock texture was observed with the Mastcam and ChemCam instruments at the Harrison target, in a large clast within a conglomerate (“Harrison” target), on sol 514 [*Sautter et al.*, 2015; *Mangold et al.*, 2016]. Harrison is composed of ~50% light-toned plagioclase phenocrysts set in a dark fine-grained matrix [*Sautter et al.*, 2015]; if Harrison is representative of the source rocks contributing to the Bradbury group, the sediment may also contain larger clasts of plagioclase and finer particles of mafic minerals. Texturally, several of the other clasts in conglomerates and possible igneous samples observed by APXS also appear to show large felsic grains intermingled with a dark mafic substrate. Compositionally, however, the clasts observed with APXS are not necessarily igneous

compositions because they may have been affected by sedimentary processes, including effects from cementation and dust cover.

The Murray mudstone, part of the Mount Sharp group, has at least a partially different provenance than the Bradbury group—the mudstone sediments have a composition that is distinct from all grain size classes in the Bradbury group. As a mudstone, like the Sheepbed mudstone, the Murray mudstone may incorporate sediment from multiple watersheds and from authigenesis within the lake itself, so the Bradbury provenance could be one of multiple contributing sources for the Murray mudstone. The elevated CIA values of the Murray suggest input from some chemically weathered source regions, but the presence of unaffected olivine and pyroxene minerals in the Murray formation suggest that the lake environment was not itself conducive to extensive mineral alteration (Figures 4.4 and 4.8). Some Murray sediments could be modeled as mixtures of primary basaltic minerals if silica was included, indicating that silica authigenesis or nearly-pure silica input by some other mechanism could have played a role in creating the Murray compositions (Figure 4.8). Other Murray sediments showed excess  $\text{Al}_2\text{O}_3$ ,  $\text{Na}_2\text{O}$ , and/or  $\text{P}_2\text{O}_5$ , which are likely components contributed by a chemically weathered source region. Further investigation of the Murray formation is required to untangle the more complex factors involved in mudstone formation, but it is sufficient for this study to recognize that the Murray unit has a distinct provenance from the Bradbury group, and should be treated independently.

#### **4.5.3.2 Influence of Sorting during Transport**

Sorting of sediment by density and grain size has long been recognized as an important process in the formation of sedimentary rocks, especially due to the economic importance of heavy mineral deposits [Mackie, 1923; citations in Weltje and von Eynatten, 2004]. Early researchers noticed that within a natural sand sample, heavy/dense minerals are concentrated in finer grain sizes and lighter minerals are found in coarser grain sizes [Rubey, 1933; Slingerland, 1977]. Rubey modeled this phenomenon using Stokes' law to describe the settling velocity (which defines particle retention in the suspended load in a flow) of particles with differing grain sizes and densities, and showed that, for example, a

spherical magnetite grain that is 0.63 mm in diameter would be suspended in the same flow as a spherical quartz grain 1.0 mm in diameter, making those two grains “hydrodynamically equivalent” [Rubey, 1933; Slingerland, 1977]. While shape and erodibility of minerals can also play a role in mineral sorting by grain size, modern surveys of different sediments show that Stokes’ law (and similar impact laws for different flow types) do quite well at describing the grain sizes of different minerals in a given mixed sediment sample based on this principle of hydrodynamic equivalence [Whitmore *et al.*, 2004; Garzanti *et al.*, 2008].

Stokes’ law and the principle of hydrodynamic equivalence explain the grain size fractions of specific minerals within a sample, but these cannot explain overall compositional trends between samples; these trends must instead be defined by the availability of grains of a given hydrodynamic equivalence within the fluvial system. That is, the overall composition is ultimately provenance dependent; if a portion of the river is accreting sediment hydrodynamically physical equivalent to 1.0 mm diameter quartz grains or 0.63 mm magnetite grains, the relative abundance of magnetite and quartz depends on the availability of those two minerals in those specific size fractions. This is dependent on the sediment provenance, the combination of abrasion and chemical weathering of the source rock before and during transport, slope and distance of transport, local flow dynamics that tend to concentrate heavy minerals in fine-grained lag deposits, introduction of additional sources, etc, which act as a system to make downstream trends in composition frequently inconsistent between locations [Johnsson and Basu, 1993]. While each system is unique, some general trends may be understood for each of these factors.

The provenance of the Bradbury group is basaltic, and at least some of the source rocks appear to have plagioclase phenocrysts in a mafic groundmass. The evidence described in this study indicates that chemical weathering does not play a major role here. Based on an analysis of grain roundness, Szabó *et al.* [2015] showed that the Gale sediments (at least those in conglomerates) have likely traveled on the order of ~50 km from their source, so Bradbury group sediments have traveled short distances relative to many sandstones on Earth. Basaltic sediment that is fluvially and not chemically weathered is difficult to find on Earth, but a few partial analogs are relevant.

The nature of sediments from similar basaltic sediment provenances are described in Fedo et al. [2015] and Nesbitt and Young [1996]. Fedo et al. crushed unweathered basalts from Kilauea, HI (porphyritic) and Cima volcanic field, CA (aphanitic) with a rock crusher to imitate impact-induced rock breakdown. They found that olivine and associated trace elements (Cr, Zn, Ni) were concentrated in fine grained fractions, while plagioclase was enriched in coarser grain fractions, and that these compositional differences between sieved grain size classes were greater for porphyritic basalt. They point out that this compositional fractionation would be enhanced during transport sorting due to significant differences in grain size and some differences in specific gravity [Fedo et al., 2015]. Nesbitt and Young [1996] studied the bulk compositions of different grain size sediments in a short (<5 km) glacio-fluvial system in Guys Bight Basin, where the bedrock is predominantly metamorphic gneiss composed of feldspars, quartz, biotite, and hornblende. The bedrock is comminuted by glacial processes and then sorted in a fluvial system, with low CIA values indicating minimal chemical weathering. Biotite and hornblende (and therefore  $\text{FeO}_T$ ,  $\text{TiO}_2$ , and  $\text{MgO}$ ) are concentrated in the muds and fine sands, whereas quartz and feldspar are relatively more abundant in medium and coarse sands, again following Bradbury group trends with mafic mineral enrichments in finer grains and felsic mineral enrichments in coarser grains [Nesbitt and Young, 1996].

The relative importance of the initial grain sizes of mineral grains (provenance) and the abrasion and breakdown of grains during transport in a fluvial system has been debated for Earth systems [e.g. Ferguson et al., 1996], and if differential abrasion played a significant role in Bradbury sediment transport dynamics it might have modified or enhanced compositional grain size signals related to provenance. Indeed, analysis of the particle shapes in Bradbury conglomerates indicate ~10-20% mass loss by physical abrasion [Szabo et al., 2015]. Physical stress tends to increase the number of monomineralic grains, thereby enhancing compositional variation with grain size if the original source rock were porphyritic [Slatt and Eyles, 1981]. So, to first-order, physical abrasion processes may have enhanced the compositional differences in Bradbury sediment grain populations.

### 4.5.3.3 Influence of Diagenesis

The Bradbury group sedimentary rocks have clearly been cemented and lithified. The Sheepbed mudstone seems to have been impermeable to sulfate-precipitating fluids that circulated through fractures, but not the fractured bedrock, during late stages of diagenesis [McLennan *et al.*, 2014; Vaniman *et al.*, 2014]. There is evidence for burial of the Bradbury and Mount Sharp groups [Schieber *et al.*, 2013; Grotzinger *et al.*, 2015], so compaction likely played a role in lithification, but further cementation is also required. The timing is constrained by late-stage calcium-sulfate-filled fractures, whose fluids did not penetrate into the surrounding rock, so the rocks must have been well-cemented prior to that fluid event [Nachon *et al.*, 2014].

The lack of open-system weathering makes it difficult to determine the composition of the cement, and it is possible that the cementing agent is distinct in different regions. There are a limited number of float rocks observed by ChemCam [Blaney *et al.*, 2014] and some observed by APXS, including float rocks Et Then and Secure [Schmidt *et al.*, 2014], that show persuasive evidence for iron oxide cements—each have >24 wt% FeO<sub>T</sub>—but these are outliers compared to other targets. The majority of targets have compositions that are consistent with primary basaltic minerals that lack evidence for open-system chemical weathering. Despite this, CheMin XRD analyses has shown that ~30% of each drilled sample is amorphous [Dehouck *et al.*, 2014; Vaniman *et al.*, 2014; Treiman *et al.*, 2015]. The amorphous component and the presence of significant amounts of phyllosilicates in the Sheepbed member together indicate closed-system chemical weathering, which would allow formation of phyllosilicates, and possible authigenetic iron oxides or salts that formed without altering the bulk composition at the scale of APXS. Compaction of phyllosilicates would help drive lithification, and salts or unstable minerals could help cement the rocks, but also could become amorphous due to desiccation and thermal cycling in the harsh Mars climate, as described in [Vaniman *et al.*, 2004].

### 4.5.4 Mechanism for Plagioclase Variation

Based on the evidence presented in this study, the major elemental variations for Bradbury rocks parallel grain size fractions and are consistent with plagioclase enrichment

in coarse grained rock units and plagioclase depletion, or mafic enrichment, in fine grained rock units (Figures 4.6 and 4.8). In the absence of evidence for open-system chemical weathering, this type of trend could relate to contributions from different source rocks and/or to mineral sorting during transport; here we investigate each of these options.

If contributions from multiple source rocks define these major trend lines, one of the source rocks must be felsic and coarse-grained, or more proximal, and another must be mafic and fine-grained, or more distal. If both petrologically-evolved felsic rocks and primitive basaltic rocks coexisted in the watershed, it would be most simple to assume that they were genetically related and both formed from the same basaltic source as magmas cooled along a liquid line of descent. If this were the case, then the endmembers of the compositional trends should correlate with magma compositions at the beginning and end of a liquid line of descent, and intermediate compositions from the liquid line of descent may be present as well. Instead, in Figure 4.7, the Bradbury group rocks show linear trends with MgO, a tracer for igneous evolution, instead of curved lines or any breaks in slope as are expected in an evolving magma, and in some cases (Figure 4.7a and 4.7h especially) the trends are steeper than would be expected from magmatic evolution alone. Furthermore, both the measured and modeled Mg#s for olivine and pyroxene minerals are consistent and do not trend with texture, so the variation between samples is related to the relative amounts of different minerals rather than the evolution of the compositions of the minerals themselves, as would be expected in an evolving magma. This implies that the compositional trends observed are not formed due to mixing of evolved and primitive magmas from the same liquid line of descent. Instead, these trends are consistent with mineral sorting from a relatively homogenous source region except for the influx of sanidine-rich material at the stratigraphic level of the Kimberley formation.

Linear trend lines showing preferential plagioclase enrichment in coarse grained materials and mafic enrichment in fine-grained materials are consistent with expected trends from comminution and sorting during transport of a porphyritic basaltic source. Physical weathering of rocks breaks the rocks down into component mineral grains which, particularly in the case of porphyritic rocks, will concentrate olivine and heavy minerals in the finest grain size fraction, and retain lithic fragments and less dense felsic grains in the

coarser grain size fraction. During transport, the finest grains remain in suspension and compositional sorting is enhanced because the feldspar grain sizes are so much larger than the mafic grain sizes that they are preferentially deposited upstream, in conglomerate facies, whereas the finer olivine and mafic grains remain in suspension until they are deposited downstream in fine-grained sandstones and lacustrine mudstones. This is consistent with the observation that the primary variations between samples are defined by their grain size and proportion of minerals, rather than the compositions of the minerals. Sorting of basaltic mineral grains during comminution and transport is the most consistent explanation for the major compositional trend in Bradbury group compositional data.

Minor trends or deviations from the principal plagioclase enrichment trend in Bradbury rocks are within expected deviations for a natural environment. The scatter around the trend is likely related to dust cover, small-scale heterogeneities in the fluvial environment, and possibly some diagenetic cementation. For example, late-stage diagenetic calcium-sulfate veins are prevalent and cause the distribution of Ca and SO<sub>3</sub> to vary from expected trends, obscuring the original ratio of high-Ca and low-Ca pyroxene.

The Sheepbed member compositions do not form the end of the trendline, but tend to sit between the fine sandstone component of the Bradbury group and the Murray formation of the Mt. Sharp group. The Sheepbed member is also the only non-fluvial, lacustrine mudstone sampled in the Bradbury group, so it has a much higher chance of incorporating sediment input from eolian or distal volcanic sources, or other fluvial sources around the crater, in addition to capturing the finest particles in the suspended load, which frequently have a more mafic composition than deposited particles. Float rocks, especially those with obscured textural features, categorized here as uncertain, also cause some of the variations from the major compositional trends and make up all of the rocks that cannot be modeled using primary basaltic components. This is expected when incorporating float rocks; these clasts could have been transported unknown distances and were frequently selected along the traverse for analysis due to their unusual appearance. Indeed, it is more surprising how clearly the trends are visible even with float rocks and outliers incorporated.

Finally, the potassium content of Bradbury group rocks is not related to the mineral sorting trends, but is instead correlated to the presence of a distinctive minor source with a

sanidine-rich composition. Mineralogical data at the Kimberley outcrop, with the highest concentration of potassium, show that the rock is still dominated by mafic minerals consistent with the main source for Bradbury group sediments, but the sanidine is separate and has an unusual characteristic high  $K_2O/Na_2O$  ratio, which is chemically inconsistent with the Bradbury provenance. The sanidine therefore is a mineralogic indicator of a distinctive protolith that contributes to at least one stratigraphic interval that is otherwise dominated by the main Bradbury group provenance.

#### **4.6 Summary**

The collection of compositional analyses on rocks of the Bradbury group in Gale Crater offers a unique dataset for sedimentary petrology because these rocks have experienced minimal cation-loss due to chemical weathering, the sedimentologic context as a fluvio-lacustrine system is generally understood, and a variety of textures and grain sizes were sampled. This dataset therefore enables us to back out information concerning the initial petrological and sedimentary processes that led to the deposition of these sediments. The principal geochemical trends for these samples reflect a concentration of plagioclase minerals in the coarsest grained samples, and a concentration of mafic minerals in the finer grained fraction. Investigation of the geochemical trends and Monte-Carlo modeling of the mineral compositions show that these trends are consistent with breakdown and segregation of plagioclase phenocrysts from a mafic groundmass during transport, and the geochemical diversity of the sediments does not require significant petrologic diversity in the sediment source region. The primary exception to this low petrologic diversity is a stratigraphic interval around the Kimberley outcrop, where high potassium sanidine must be contributed by a unique source rock that only periodically contributes sediment to the Gale Crater basin. The formation of the Bradbury group from a relatively homogeneous, unweathered basaltic provenance provides contrast and background for understanding of higher layers on Mount Sharp.